Designing Magnesium-Selective Ligands Using Coordination Chemistry Principles

Edward R. H. Walter,* [a] Christopher Hogg,[b] David Parker[b] and J. A. Gareth Williams[b]

[a] Department of Chemistry, Imperial College London, Molecular Sciences Research Hub, White City Campus, Wood Lane, London, W12 0BZ, UK

[b] Department of Chemistry, Durham University, Durham, DH1 3LE, UK.

Abstract

Progress in the selective binding and detection of magnesium ions has been slower than other biologically important divalent metal ions like calcium and zinc. The most widely used ligands for Mg^{2+} are by no means optimal, as they are not selective for it. Nevertheless, Mg^{2+} is a major cation in all cells, with physiologically critical functions. There is a need for improved sensors for Mg^{2+}. In this review, we consider how an appreciation of fundamental coordination chemistry principles may inform the development of new ligands for Mg^{2+}. A number of representative examples of ligands of differing denticity are discussed in this context. Low-denticity ligands such as β-keto acids offer the best selectivities, but speciation is an issue as other polydentate ligands such as pyrophosphate may complete the coordination sphere. High-denticity ligands based on aminocarboxylates such as APTRA typically offer the highest stability constants, but they bind Ca^{2+} and Zn^{2+} more strongly than Mg^{2+}. We highlight recent examples featuring related aminophosphinates, where the longer bonds and smaller bite angles favour selectivity towards Mg^{2+}. Macrocylic receptors for magnesium are not discussed explicitly.

Keywords: Magnesium; ligand design; selectivity; sensing; fluorescence spectroscopy; fluorescence imaging.

* Corresponding author. E-mail address: e.walter@imperial.ac.uk

1. Introduction

Magnesium is the second most abundant divalent cation in the body, with total concentrations in mammalian cells normally in the range 14 – 20 mM [1]. Most cellular Mg^{2+} is bound to adenosine triphosphate (ATP), polyphosphates and pyrophosphates, in the mitochondria and endoplasmic reticulum in particular, such that the concentration of the 'free' Mg^{2+} ion is much lower, typically around 0.8 – 1.5 mM[§] [2–4]. The distinction between 'free' (ionisable) and bound magnesium is rather arbitrary, and should be considered with respect to its intracellular compartmental distribution.

Magnesium ions have a number of key fundamental roles within cells, for example, stabilising the structure of DNA [5,6] and controlling the conformation of nucleic acids and proteins [7]. Mg^{2+} is established as an essential co-factor in over 600 enzymatic reactions [8], either directly or by substrate modification on binding [9]. Of particular importance is the activation of ATPase, a process that is crucial for the generation of energy within cells. The mis-regulation of Mg^{2+} concentrations in serum is also known to correlate with a number of severe health conditions. For example, Mg^{2+} deficiency and the onset of hypomagnesemia, is linked to a range of cardiovascular [10], neurodegenerative [11,12] and renal diseases [13]. Elevated magnesium concentrations, or hypermagnesemia, is significantly less widespread, but has been linked to muscle weakness and fatigue [8].

Over many years, only slow progress has been made in developing methods for the selective detection of Mg^{2+}. Hasselbach first published work indicating the importance of magnesium ions within cells in 1957 [14] and yet, over half a century later, still very little is known about the homeostasis of Mg^{2+}. The slow pace of advances in selective detection of Mg^{2+} led Wolf and co-workers to label it the 'forgotten cation' in a review in 2010 [15]. Other biologically relevant cations such as Ca^{2+}, H_3O^+, Na^+ and Zn^{2+} have been studied in far greater depth, unlocking detailed information on transportation and homeostasis in mammalian cells.

In order for more information to be gained on Mg^{2+} homeostasis, more sensitive and selective methods are required for its detection and quantification. Analytical methods such as atomic absorption spectroscopy (AAS) are inaccurate and impractical at the cellular and

§ The use of the word 'free' (also termed 'labile' in some instances) here denotes cations that are hydrated but, importantly, not bound to biomolecules or assemblies such as nuclei acids or phospholipids where Mg^{2+} fulfils a structural role. 'Free' cations may have the ability to move between biological compartments, including cells and organelles. 'Free' Mg^{2+} is typically found in the range 0.5 to 2 mM and such a value is typical of its concentration in the cytoplasm and endoplasmic reticulum.

sub-cellular level. Meanwhile, the use of isotopically enriched magnesium (^{25}Mg and ^{26}Mg are stable, along with the main isotope ^{24}Mg) offers promise but requires sophisticated mass spectrometry techniques, such as ICP-MS, to improve the accuracy of results [16], whilst tracer work with radioactive ^{28}Mg is limited to appropriately accredited laboratories.

Since the 1980s in studies initiated by pioneers such as Roger Tsien, the development of luminescent probes has revolutionised understanding of the role of Ca^{2+} ions in cell biology. The design of analogous probes for Mg^{2+} has the potential to transform knowledge of magnesium in a similar manner. But, progress has been slower and selectivity for magnesium over calcium in particular remains the greatest challenge. Many of the current clinically available probes based on pentadentate ligands have selectivity issues with competing divalent cations, including Ca^{2+} and Zn^{2+}, while more recent alternative probes of lower denticity are subject to competition with Mg–ATP^{2-} and related phospho-anion complexes limiting their scope for biomedical application [17].

A cursory literature search rapidly reveals that there is rather little variation in ligand design regarding Mg^{2+} binding chelates. The novelty in new sensors has hitherto typically come from modifications to the parent chromophore, or the use of different fluorophores to improve the photophysical properties. More work on the metal-binding unit is imperative if new, more selective Mg^{2+} binding probes are to be developed successfully.

An informative and accessible recent review from Buccella and Lazarou outlines a number of the key and pressing issues that surround the quest for a greater understanding of the role of Mg^{2+} in cell signalling [18]. Here, in contrast, we seek to outline recent developments towards the design and synthesis of new binding chelates and luminescent probes to bind and signal Mg^{2+} selectively. Of particular importance is the consideration of fundamental and sometimes overlooked coordination chemistry principles to improve the selectivity of metal ion binding.

2. Ligand Design Principles

In order to design ligands that bind metal ions selectively and with a suitable affinity profile, a number of important factors need to be considered. Fundamental principles of coordination chemistry, such as the Hard-Soft Acid-Base (HSAB) principle, coordination number preference, and the chelate effect, provide a starting point in the development of new and improved probes for Mg^{2+}. Of course, there are other factors to be considered too, one of

which is pH response – or rather the lack thereof. It is highly desirable for the probe to show no changes with pH variation over the physiological range of 6 – 8 (and lower for some organelles such as lysosomes [19]), otherwise additional controls have to be introduced. Salient photophysical considerations concerning the incorporation of the luminescent reporter group are discussed at the end of this section.

2.1 Sensitivity and Selectivity of Metal Ion Binding

The position of the equilibrium between a ligand L and metal cation M is quantified by a binding constant. In the literature, both association (K_a) and dissociation (K_d) constants are used when discussing ligand binding. An expression of K_d, as well as its relationship to K_a, is shown in **Eq. 1**. Spectroscopic outputs, such as the emission intensity of the reporter group of a luminescent sensor, will be at least approximately proportional to the mole fraction of the bound form, ML, that is present at given concentration of [M] [20]. A K_d value in the same range as the concentration of target metal ion (for example ~ 50 mM in **Fig. 1** *green*) is required to measure fluxes accurately. When K_d >> [M] or K_d << [M] the spectroscopic output will be essentially invariant with changes in [M] (**Fig.1** *blue* and *red*). However, it should be noted that ligands in the latter regime, or even with irreversible binding, may still have application as a 'chemodosimeter' [21].

$$K_d = \frac{[M][L]}{[ML]} = \frac{1}{K_a} \quad \textbf{(Eq. 1)}$$

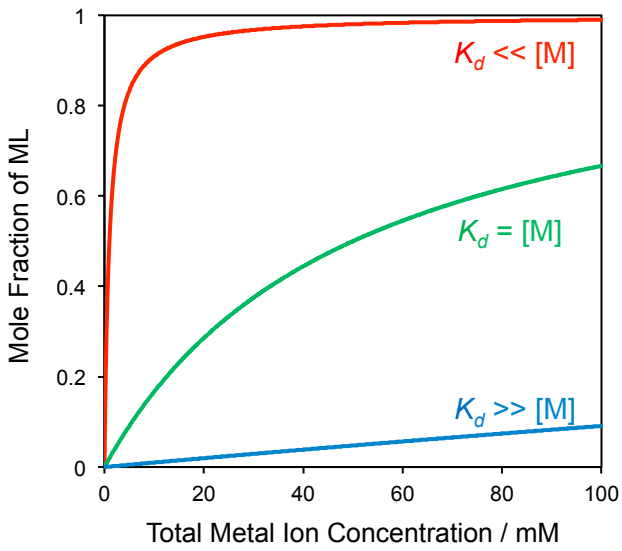

Fig. 1. Binding isotherms for a 1:1 metal (M) to ligand (L) binding system with various K_d values.

Not only should a sensor have an appropriate K_d value, comparable to the concentration of metal ions [M] under investigation, it should also be *selective* for the target metal ion, since samples for analysis typically contain numerous different metal ions. In terms of cell biology applications, for example, the sensor should not respond to other metal ions at their prevailing cellular concentrations. We shall consider some of the approaches that allow tuning of the sensitivity and selectivity of ligand chelates for this purpose.

2.2 Choice of Donor Group

The choice of the donor or ligating group is usually the starting point for ligand design, and is a critical consideration in order to form stable metal complexes. In the 1960s, Pearson developed the HSAB principle, proposing that anions and neutral lone pair donors (Lewis bases) and cations (acids in the Lewis definition) could be divided into "hard" and "soft" categories (**Table 1**) [22,23]. Hard bases will bind favourably with hard acids; soft with soft. Hard acids and bases are considered to be of low polarisability, for example, small, charge dense ions often with a high formal charge. In contrast, soft acids and bases display the opposite characteristics. More promiscuous ions, which show affinity to both hard and soft ions, are referred to as "borderline". The HSAB principle has proved to be a remarkably useful starting point for further tuning and refining the design of ligands to enhance selectivity. The right choice of ligand donor can significantly improve binding selectivity and thermodynamic stability of the complexes formed. Choosing the 'wrong' donor group is likely to have a detrimental effect on metal ion selectivity and affinity. It is relatively straightforward to discriminate between hard and soft acids by changing the ligand donor groups. However, differentiating between multiple hard acids or soft acids is more challenging: other properties of the metal ions then need to be considered, such as size, polarisability and preferred coordination number.

Table 1 Examples of hard and soft acids (metal ions) and bases (neutral and anionic ligands) [22,23].

	Hard	**Soft**	**Borderline**
Acids (Metal ions)	Li^+, Na^+, Mg^{2+}, Ca^{2+}	Cu^+, Ag^+, Pd^{2+}, Pt^{2+}	Zn^{2+}, Fe^{2+}, Co^{2+}, Ni^{2+}
Bases (Ligands)	F^-, Cl^-, H_2O, $-COO^-$, HPO_4^{2-}, NH_3, $R-NH_2$	I^-, HS^-, CN^-, PR_3	Br^-, NO_2^-, SO_3^{2-}

2.3 The Chelate Effect and Chelate Ring Size

The “chelate effect” refers to the increased thermodynamic stability of metal complexes with a polydentate ligand over an analogous complex where each donor atom is provided by a monodentate ligand. Such a simple definition is often sufficient, although more thorough definitions have been proposed [24]. The origin of the chelate effect in aqueous solution is commonly attributed to a large increase in the translational entropy of the system upon binding of a chelating ligand, due to the expulsion of the water molecules of the hydrated metal ion [25]. In reality, the effect is more nuanced, as additional entropic factors based on vibration, rotation, solvation, symmetry and the number of isomers available to a complex are also important [26]. Indeed, the entropic change may be less favourable than appears from the simple picture of water expulsion. Flexible ligands will often have access to many conformations in their unbound form, but are generally restricted to a smaller subset when bound to a metal ion, reducing the entropic favourability of complexation. In 1988, Cram stated that “pre-organisation is a central determinant of binding power” [27], describing in detail how more rigid ligands give rise to larger association constants compared to their flexible analogues. Enthalpic considerations of the chelate effect should not be neglected though, as they can be harnessed to provide a method for tuning metal ion selectivity (**Section 2.4** and **2.5**). The use of macrocyclic ligands will not be discussed here in the since the application of aza-crown ethers, for example, as probes for Group 1 and 2 metal ions in solvents of differing polarity, has been extensively covered in recent reviews [28,29]. In the case of Mg^{2+} binding, quinolyl-substituted diaza-crown ethers have shown some promise and typically display K_d values in the μM range, making them appropriate to measure total free magnesium intracellular concentrations. These analyses offer modulation of the rather weak fluorescence emission intensity and require both the cell sample to be lysed and the use of methanol as a co-solvent in the measurement [30].

Five and Six-Membered Chelate Ring Formation

It is well known that increasing the chelate ring size from 5 to 6 decreases complex stability, but it is often overlooked that the extent of this decrease depends on the size of the metal ion. Generally, increasing the chelate ring size from 5 to 6 will destabilise complexes with larger metal ions more than smaller ones [31,32]. Such an observation is shown graphically for selected multidentate ligands in **Fig. 2**.[¶]

[¶] Ethylenediamine (EN), Trimethylenediamine (TN), Bipyridine (BPY), DPYA (2,2’-Dipyridylamine), Ethylenediaminetetracetic acid (EDTA) and Trimethylenediamine-N,N,N’,N’-tetraacetic acid (TMDTA).

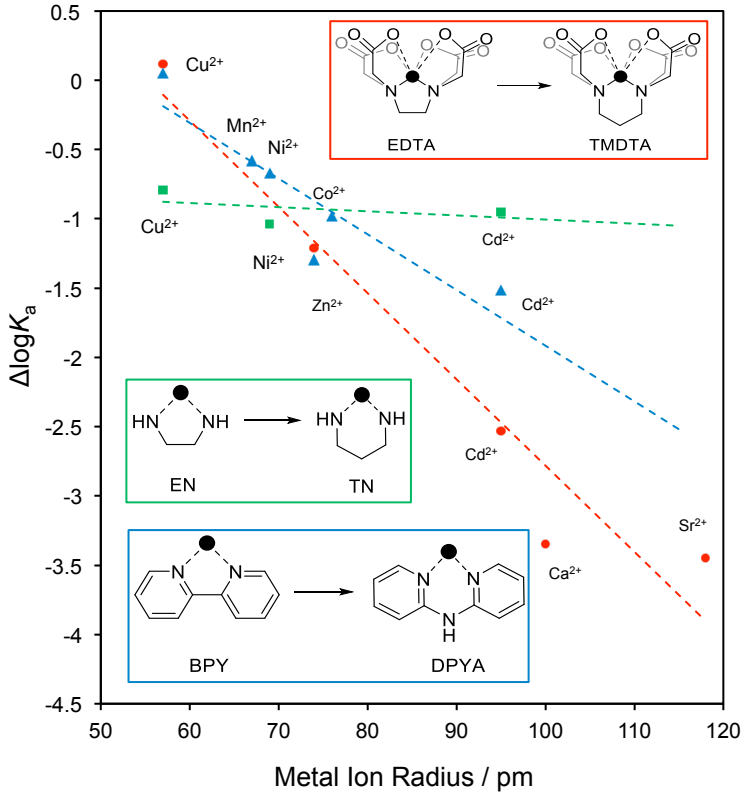

Fig. 2. The change in log K_a on going from a 5-membered chelate ring to an analogous 6-membered chelate shown as function of metal ion radius [32–34]. EDTA vs TMDTA is shown in *red* circles, BPY vs DPYA in *blue* triangles and EN vs TN in *green* squares. I = 0.1 M and T = 25 °C (in some cases, values have been corrected from 20 °C to 25 °C) [35].

Using EN and TN as examples, the phenomenon of chelate ring size may be understood by considering the bond lengths and angles adopted in the minimum strain energy conformations of 5- and 6-membered chelate rings (**Fig. 3**). The 5-membered chelate, adopting a distorted half-chair-like conformation, displays longer M–N bonds and a smaller N–M–N bite angle compared to the 6-membered chelate. The latter experiences minimum strain in a chair conformation similar to that of cyclohexane.

Given that larger metal ions are more amenable to longer M–N bonds and typically have higher coordination numbers, they prefer smaller bite angles. And so, a large increase in unfavourable strain energy on moving from a 5- to 6-membered chelate ring is likely for large metal ions. The enthalpy of binding for large metal ions is thus expected to be much less favourable for 6-membered chelate rings than 5-membered ones. Such a statement is

supported both by experimental data [32,35] and by values estimated by DFT [36]. Conversely, smaller metal ions will be more suited to the shorter bonds and larger bond angles required to minimise strain energy in the 6-membered chelate, so the reduction in the enthalpy of binding is much less on moving from a 5- to a 6-membered chelate.

Furthermore, the change in K_a on increase in chelate ring size from 5 to 6 is far more dramatic for rigid ligands and/or ligands of higher denticity. The effect is very small for EN vs TN, whilst it is much larger for BPY vs DPYA and EDTA vs TMDTA (**Fig. 2)** [32,35,37]. Such a change is consistent with the interpretation that the effect is based on changes in strain energy in the complex, as one would expect that complexes of more rigid / polydentate ligands would be far less accommodating of deviations from the minimum strain energy values shown in **Fig. 3**.

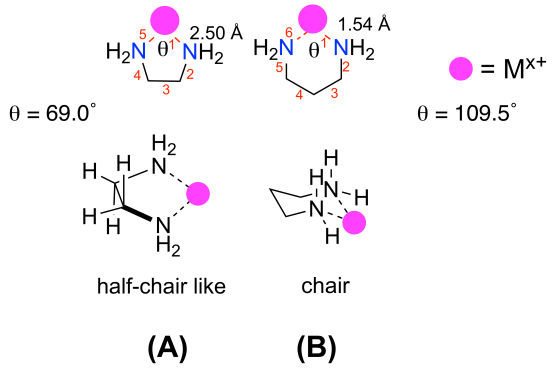

Fig. 3. The minimum strain energy conformations of **(A)** 5-memebered, and **(B)** 6-membered ring chelate on binding of metal ions (in *black*) formed on the coordination of EN and TN with metal ions (in *pink*). 3-Dimensional representations of the structures are also shown (bottom).

A recent review (2019) of complexes containing the bidentate ligands PHEN, BPY and EN in the Cambridge Structural Database (CSD) has shown that an increase of the metal ion radius results in a decrease in the angle of the N–M–N bite angle with elongation of the M–N bond lengths [38]. The trend holds firm for the 3d elements in particular. Some larger cations, such as La^{3+} and Hg^{2+}, have been found not to fit the trend though, so some caution is required when generalising that larger metal ions favour the formation of 5-membered ring chelates [38]. *Nevertheless, introduction of a 6-membered chelate ring is a useful tool likely to increase the selectivity of a ligand towards smaller metal ions.*

2.4 Ligand Denticity

The use of chelating and macrocyclic ligands not only offers a way to increase binding strength, but can also provide a method for tuning the selectivity of the ligand. Increasing the ligand denticity is often thought to lead to an increase in complex stability [25]. However, there are examples where *decreasing* the ligand denticity inherently increases the stability of complexes with smaller cations [39]. For example, the removal of three neutral oxygen donors on going from diethylenetrioxydiacetate (DETODA) to oxalate decreases the log K_a values of larger metal ions, such as Sr^{2+}, whilst increasing the log K_a values of smaller metal ions, such as Cu^{2+} (**Fig. 4**).

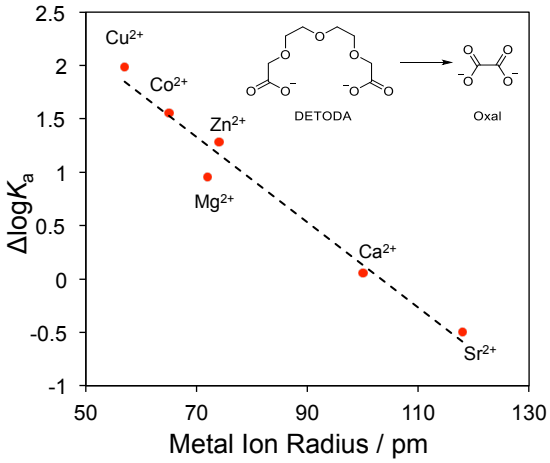

Fig. 4. The change in log K_a on going from the ML complex of diethylenetrioxydiacetate (DETODA) to oxalate (Oxal) as a function of metal ion radius; I = 0.1 M, T = 25 °C [32,34,35].

Changing ligand denticity will affect the enthalpies and entropies of metal ion binding. There is likely to be a similar, smaller entropic gain in the system for both small and large cations on going from a ligand with higher denticity to one with lower denticity. However, smaller cations can suffer enthalpic penalties when binding to high denticity ligands, due to steric crowding around the small metal centre. So, for smaller ions, reducing the denticity may actually lead to a more favourable enthalpy of binding that outweighs the decrease in the entropy of binding. Conversely, for larger metal ions – which are less likely to encounter such steric challenges – there is likely to be much less of a change in the binding enthalpy

on moving from higher to lower denticity [32]. Reducing ligand denticity may thus offer one method for favouring selectivity towards smaller metal ions over larger ones.

2.5 Photophysical Aspects in Luminescent Probe Design

In addition to ligand design, it is also necessary to consider the properties of the luminescent reporter group and the nature of signal transduction on binding.

2.6.1 Desirable Photophysical Characteristics

The choice of luminescent reporter group for a biological application is an important one. Low energy excitation is desirable, increasing the tissue penetration of light for optical imaging due to the lower absorbance of endogenous biomolecules. High energy excitation (e.g. in the UV or violet/blue regions), can cause intracellular damage through the formation of reactive oxygen species (ROS) [40], limiting their widespread application. Probes that not only satisfy this requirement, but also have large molar extinction coefficients (ε), high luminescence quantum yields (Φ_{lum}) and excellent photostability, are highly desirable.

The use of luminophores with a large Stokes' shift (the relative energy difference between the absorbance and emission of light) is also preferable. In many organic fluorophores, the energy difference is small, attributable mainly to the reorganisation of solvent molecules around the excited state molecule. Significant overlap of absorption and emission spectra can result in problems such as self-absorption, where emitted light is reabsorbed by ground-state molecules [41]. Phosphorescent metal complexes that emit from triplet states have intrinsically larger differences between absorption and emission energy, as does the sensitised emission of lanthanide ions.

2.6.2 Signal Transduction

Recognition of a binding event is often achieved by one of two methods, either a perturbation of an internal charge transfer (ICT) excited state (**Fig. 5A**) or the inhibition of non-radiative decay by photoinduced electron transfer (PeT) (**Fig. 5B**) [42]. Fluorescence Resonance Energy Transfer (FRET) can also be used to quantify binding events [43–45], but no such probes appear to have been synthesised for Mg^{2+} to date.

ICT-based sensors are perhaps the most utilised for the binding of metal ions and rely upon a "push-pull" energy transfer mechanism from an electron donor to an electron acceptor moiety. Such a process is most commonly achieved by directly conjugating one or more of

the ligating atoms with the aromatic reporter group, making a significant contribution to the frontier molecular orbitals of the molecule. Upon binding of a metal ion, the charge transfer from the donor atom is reduced significantly and a hypsochromic (blue) spectral shift is typically observed. Such a shift in wavelength, often observed in the excitation spectrum, enables binding events to be measured ratiometrically by monitoring the multiple excitation wavelengths and calculating the ratios of the subsequent intensity outputs (**Fig. 5A**). Comparing two (or more) wavelengths is particularly advantageous as it eliminates discrepancies in the degree of cell uptake and cell extrusion of the sensor, or fluctuations in light intensity at the observation point [46].However, it should be noted that, unlike the ideal case thus far described, in many instances the wavelength spectral shifts involved are small, such that only an intensity change of a single peak is observed. In this scenario, ratiometric measurements are not possible and quantitative metal ion concentration determination can only be achieved if additional factors such as ligand concentration are known.

Luminescent sensors that work on the basis of a PET sensing mechanism are very different, and tend not to be appropriate for ratiometric sensing. The binding chelate is commonly a separate, discrete entity from the luminescent reporter and so has little influence on the relevant ground and excited state energies of the probe. Instead, PET offers a route to a non-radiative decay process by luminescence quenching, either in the unbound or bound state, causing a “turn-on” (reductive PET inhibited upon cation binding) or “turn-off” (oxidative PET is promoted on cation binding) response in the emission respectively (**Fig. 5B**). Due to its “turn-off” nature, oxidative PET is less desirable and binding is more difficult to quantify [47,48]. Our focus in this review is on ligand design, so for a more detailed evaluation of luminescent reporter groups and explanation of signal transduction mechanisms, we direct the reader to two recent reviews [49,50].

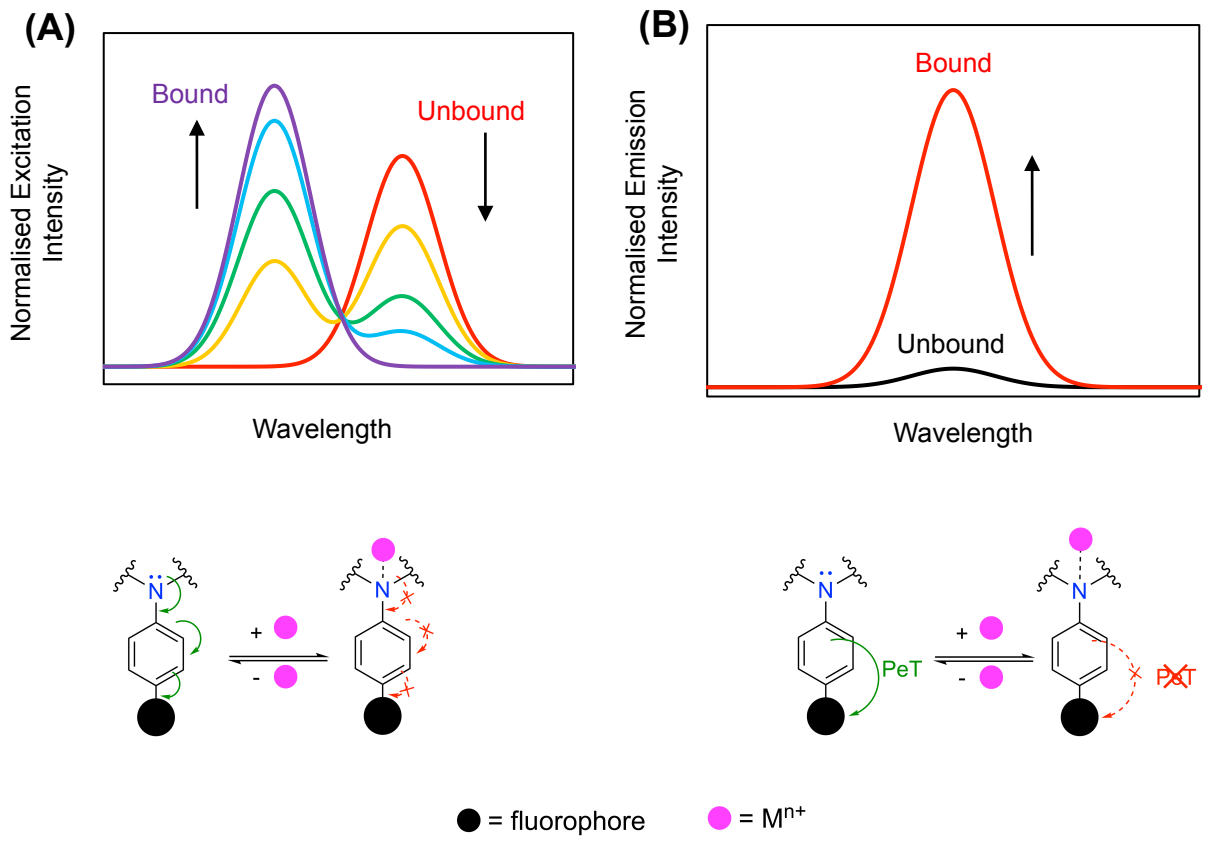

Fig. 5. Showing **(A)** the perturbation of an ICT excited state with a characteristic hypsochromic shift in the excitation spectrum and **(B)** a 'turn-on' reductive PET mechanism following metal ion binding.

2.6.3 Biochemical Considerations

If a molecular probe is to be utilised in a biological setting, there are a number of other technical aspects to be considered. One such consideration is the delivery of the probe to the cell. Ideally, for passive diffusion into the cell, the probe should be sufficiently polar to be water soluble but lipophilic enough to pass through the membrane. This is potentially problematic for many metal ion probes, particularly for hard cations, as the presence of anionic donors such as the carboxylate group often hinders diffusion across the cell membrane. To counteract this issue when developing sensors for Ca^{2+}, Tsien and colleagues synthesised the acetoxymethyl (AM) ester of BAPTA – a kind of pro-drug approach to cellular imaging [51]. The AM ester confers a suitable lipophilicity to the probe so that it can cross the plasma membrane and, once the AM functionalised probe enters the cell, esterases hydrolyse the ester to the free carboxylate. The sensor, now being anionic, cannot readily leave the cell through passive diffusion (though it can be extruded through

other pathways). Utilisation of the AM ester to concentrate sensors in cells is now a popular method for sensors containing carboxylate units, as passive diffusion is less intrusive than methods such as microinjection [52].

Beyond achieving entry to the cell, it may also be desirable for the sensor to localise into a particular compartment. Though not fully understood, this can often by achieved by appending the sensor with a certain functional group or vector. It can be as simple as a triphenylphosphonium cation for mitochondrial localisation, or more complex, e.g. using a particular peptide [53]. When designing a sensor, it is important to keep this in mind, as candidates that show promise in preliminary cellular studies should ideally be able to be modified further to allow targeting to a desired organelle. A final point to note is that the sensor should be non-cytotoxic (or have only low cytotoxicity) both in the ground and excited states.

2.7 Designing Selective Probes for Mg^{2+} ions

The principles discussed above can be applied to the selective coordination of any particular metal ion in aqueous media, but specifically with regards to Mg^{2+}, they are important to consider in order to develop more selective probes. Since 'free' Mg^{2+} in most cells is in the range 0.8 – 1.5 mM, ligands should be designed with $K_d \sim 1$ mM to provide an appropriate sensitivity. Mg^{2+} is a small (ionic radius is 72 pm in coordination number six) [25], non-polarisable, hard divalent cation that forms its more stable complexes with hard ligands containing oxygen and / or nitrogen donor groups. Binding selectivity over softer cations can be easily achieved through choice of the ligand donor groups. For example, Cu^{+} ions are considerably softer and favour the binding of soft ligand chelates such as thioether functionalised systems (**Table 1**, **Section 2.2**) [54]. Selectivity for Mg^{2+} over Cu^{+} is thus readily achievable.

However, Ca^{2+} and Zn^{2+} are the main competing divalent cations for Mg^{2+} *in vivo*. Ca^{2+} is also a hard acid, favouring binding to oxygen and nitrogen donor groups, such as carboxylates and amines. Considering the donor group only is, therefore, not enough and other properties of the cations need to be considered. Ca^{2+} is much larger than Mg^{2+} (typical ionic radius of Ca^{2+} is 100 pm in coordination number six and 112 pm in coordination number eight) [34], offering the possibility to tune the binding by changing the ligand chelate ring size and denticity (**Section 2.4** and **2.5**). In contrast, gaining selectivity over Zn^{2+} by methods based on size alone is difficult due to the similarity in size of Mg^{2+} and Zn^{2+} (typical ionic

radius of Zn^{2+} is 74 pm in coordination number six [34]). Strategies based around varying the identity of donor groups will be more successful, as Zn^{2+} is a borderline cation in the HSAB categorisation. In its interactions with ligand donors, Zn^{2+} has a greater degree of covalency than Mg^{2+}, in part associated with the poorer shielding of nuclear charge afforded by the 3d electrons.

Many chelates for Mg^{2+} are based on the pentadentate *o*-aminophenol-*N,N,O*-triacetic acid (APTRA) framework or bidentate *β*-keto acids. The relative merits of these high and lower denticity approaches are discussed in detailed in **Sections 3** and **4** respectively. To reduce the competitive binding of Ca^{2+} and Zn^{2+}, it is thought that a lower denticity could be favourable. Insightful work by Buccella and co-workers on the APTRA ligand, has found that there is a large enthalpic penalty (thought to be due to differences in the hydrated complexes) but also a large entropic gain for the binding of Mg^{2+} [55]. For the larger Ca^{2+}, this enthalpic penalty is much smaller, with entropy the underlying factor to consider. The binding constant will simply decrease in accordance with the smaller entropic gain upon changing to a lower denticity ligand. In contrast, the binding of Mg^{2+} to a ligand of lower denticity would result in a smaller change in the binding constant. In this case, the decrease in the enthalpy penalty would be offset by the decrease of the entropy of binding. Such an investigation provides evidence that a higher binding selectivity for a smaller metal ion can be achieved by lowering the denticity of a ligand [55].

The presence of other potentially ligating molecules in significant concentrations in some organelles – and which can compete with or complement the coordination offered by the probe – should be considered too. Mg^{2+} binds strongest to key enzymes like ATPase and ATP-synthetase ($K_a = 10^8\ M^{-1}$), and is the major counterion associated with DNA and RNA. In cell walls, teichoic acid – based on a glycerol phosphate backbone – binds Mg^{2+} strongly. Relatively strong 1:1 complexes are formed with ATP, GTP and pyrophosphate (range 10^4 to $10^6\ M^{-1}$), but these complexes are of modest kinetic stability, with dissociation rates of the order of 10^3 to $10^4\ s^{-1}$, such that 'free' phosphate units become available.

With ligands of lower denticity, the Mg^{2+} ion is coordinatively unsaturated and the formation of complexes of differing speciation must therefore be considered, where bound waters in aqueous media are replaced by other ligating species. With bi- and tridentate ligands for example, Mg^{2+} will also form ML_2 complexes, and more critically complexes of the type MgLX, where X is OH (from hydrolysis of a coordinated water) or represents a polydentate anion. In a cellular environment, the large range of phosphorus oxyanions – such as those listed above – must be considered. The pertinent stability constants listed in **Table 2** make

the point clearly. The formation of ternary anion adducts is seldom considered in much published work, and a naïve assumption of simple MgL formation is often invoked. Thus, although reducing ligand denticity does offer a means of favouring selectivity towards smaller ions like Mg^{2+}, due consideration must be given to ternary complex formation.

Table 2 Stability Constant Data for Magnesium Anionic Complexes.

	ATP [56]	ADP [56]	pyrophosphate [57]	citrate [58]
log K_{MgL}	4.72	4.11	5.41	3.31
log K_{MgLH}	2.79	2.94	3.06	4.09

In summary, the following methods emerge to aid the design of selective chelates for Mg^{2+}:

1. Harder donor atoms will favour the binding of harder metals. Since Mg^{2+} is a hard polarising cation, prospective ligands will need to feature hard donor groups.
2. Ligands of lower denticity could allow for more selective binding of Mg^{2+} over Ca^{2+}. Low denticity can, however, cause additional complications through ternary complex formation (**Sections 4** and **5**).
3. The incorporation of 6-membered chelate rings in place of 5-membered ones will increase selectivity for Mg^{2+} over Ca^{2+} due to the difference in ionic radius.

In subsequent sections, we discuss the effect of lowering the ligand denticity in an attempt to bind the smaller Mg^{2+} ion more selectively, with accompanying literature examples. An alternative approach will also be discussed, namely increasing the dimensions of the chelate ring around Mg^{2+} through the use of phosphinate as opposed to carboxylate ligands (**Section 3.2**).

3. Pentadentate Ligands

Pentadentate ligands were the first binding chelates developed in an attempt to understand Mg^{2+} homeostasis in greater detail. Research has predominantly focused on aminocarboxylate ligands such as *o*-aminophenol-*N,N,O*-triacetic acid, APTRA (**Fig. 6C**), but recent work has introduced the phosphinate analogue, *o*-aminophenol-*N,N*-diacetate-*O*-methylene-methylphosphinate, APDAP (**Section 3.2**). Both APTRA and APDAP contain five hard ligating atoms (N and O), which are expected to form four 5-membered chelates [5,5,5,5] around divalent metal ions (illustrated for APTRA in **Fig. 6C**).

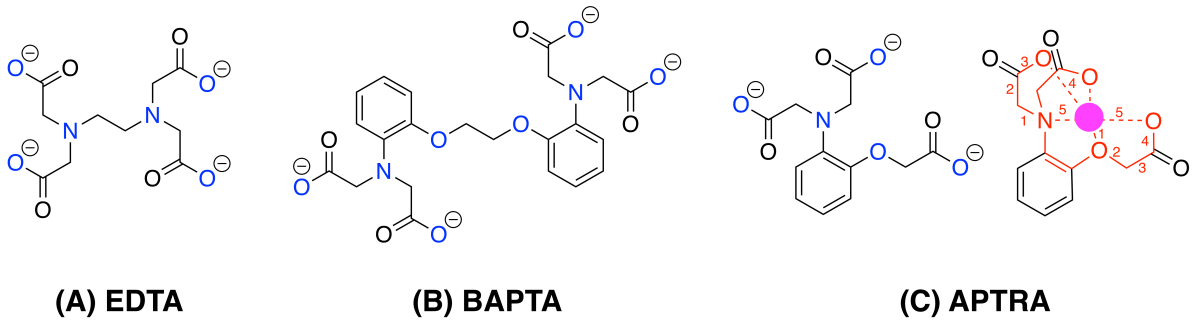

(A) EDTA **(B) BAPTA** **(C) APTRA**

Fig. 6. The structures of **(A)** EDTA, **(B)** BAPTA and **(C)** APTRA. The formation of a [5,5,5,5] complex upon binding a metal ion is illustrated for APTRA. Binding groups in the free ligands are highlighted in blue.

3.1 Carboxylate Ligands – APTRA

The combination of amine and carboxylate groups separated by a single carbon atom is ubiquitous amongst ligands used for the binding of Group 2 and hard transition metal ions. Ethylenediaminetetraacetic acid, EDTA (**Fig. 6A**), for example, is used to sequester metal ions and inhibit bacterial growth in a vast array of consumer products [59], while the work of Tsien and co-workers led to BAPTA [60] and Fura-2 [61]. BAPTA (**Fig. 6B**) is an octadentate chelator that forms seven 5-membered rings around metal ions, binding Ca^{2+} with an extremely high affinity and with good selectivity. Detailed homeostatic information is known about Ca^{2+} and its crucial role in cell signalling thanks to these chelators [51].

The smaller Mg^{2+} ion, in comparison, received much less attention. A major advance can be traced to the development of pentadentate *o*-aminophenol-*N,N,O*-triacetic acid (APTRA, **Fig. 6C**) by London and co-workers in the late 1980s to measure 'free' Mg^{2+} in the cytosol by ^{19}F NMR experiments [62]. APTRA, an analogue of EDTA, is a lower denticity cousin of BAPTA that forms four 5-membered chelate rings with metal ions, denoted a [5,5,5,5] chelate. It was hypothesised that a lower denticity compared to the octadentate BAPTA would inherently favour the binding of the smaller Mg^{2+} ion.

FURAPTRA, or **Mag-Fura-2**, was the first fluorescent probe reported to detect the binding of Mg^{2+} (**Fig. 7A**). It incorporates the APTRA chelate into a fluorescent aromatic moiety to allow transduction of the metal binding event into an optical signal. Structurally analogous to **Fura-2**, **Mag-Fura-2** has a K_d of 1.5 mM in HEPES buffer and was first used to quantify a cytosolic Mg^{2+} concentration of 0.59 mM in isolated rat hepatocytes [63]. Although it was determined that **Mag-Fura-2** displayed a higher affinity for Ca^{2+} ($K_d = 53\ \mu M$), the concentration of 'free' Ca^{2+} in most cells is two to three orders of magnitude lower, in the

high nM (or low μM) range [63,64]. Such an affinity introduces a number of significant challenges when attempting to quantify 'free' Mg^{2+} concentrations in cellular compartments where Ca^{2+} ions are above basal levels. For example, the endoplasmic reticulum, Golgi apparatus, and serum have 'free' Ca^{2+} in the low mM (or high μM) range [65–67]. In the Golgi apparatus Mg^{2+} is believed to be present in much lower concentrations, but as organelle selective probes are not yet available, data on the resting concentrations and flux of the Mg ion to and from these organelles is lacking. Complications could also arise when monitoring the flux of 'free' Mg^{2+} in cells, as Ca^{2+} fluctuations can result in higher cellular concentrations above basal levels [64]. The higher affinity for Ca^{2+} vs Mg^{2+} is due to a number of factors, but a likely contribution is the preference of the larger Ca^{2+} ion to form 5-membered ring chelates (**Section 2.4**).

A further limitation is that the commercially available, first-generation APTRA sensors, **Mag-Fura-2 and MagIndo-1** (absorption λ_{max} = 369 and 349 nm respectively) [62,67] have relatively short excitation and emission wavelengths, limiting their application. The report of **Nap.APTRA** (**Fig. 7E**) in 2001 was seen as an alternative synthetic pathway to introduce a range of polyaromatic groups into the APTRA binding chelate [69]. In buffered solutions (pH = 7.2, 16 μM), naphthalene-based **Nap.APTRA** was found to act as a 'turn-on' ratiometric probe in the presence of Mg^{2+}, with a 7-fold increase in the fluorescence intensity at 358 nm and a 1.8-fold increase observed at 499 nm. A 30 nm blue-shift in the excitation spectrum was observed on Mg^{2+} binding, due to the elimination of ICT from the lone pair of electrons on the aniline nitrogen atom into the aromatic reporter group (**Section 2.6.2**) [69]. Such a response is characteristic of *para*-substituted aniline probes of this nature [60,61,70].

More recently, second generation APTRA-based systems have been developed to enable longer-wavelength excitation and emission. Buccella and co-workers have developed a range of APTRA sensors that possess excitation wavelengths more suitable to live fluorescence imaging applications. The incorporation of heavier chalcogens (S, Se) in place of the oxygen atom in the structure of **Mag-Fura-2** (e.g. **Mag-S**, **Fig. 7B**) resulted in a larger Stokes' shift between the unbound and metal-bound states of the aromatic reporter group. The largest bathochromic shift in the unbound state was reported for **Mag-Se** (**Fig. 7C**) with an excitation maximum of 412 nm and an emission maximum of 584 nm, significantly red-shifted compared to 369 nm and 511 nm respectively for **Mag-Fura-2** [71].

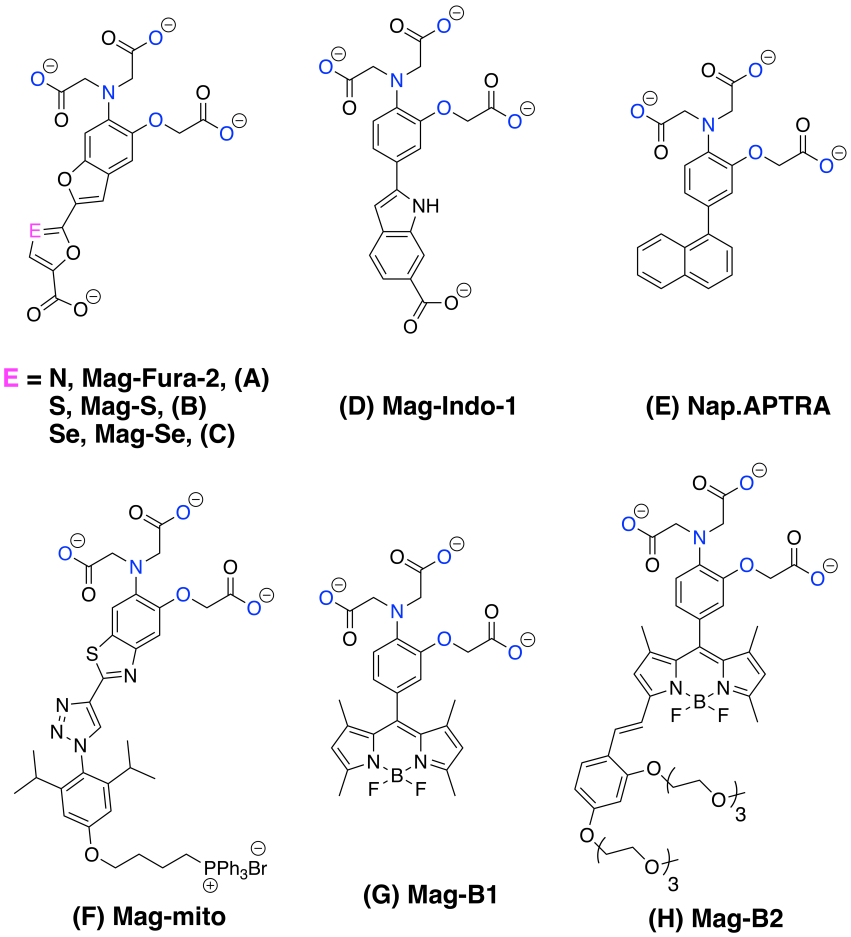

Fig. 7. The structures of first and second generation of APTRA analogues discussed in this review. Binding groups are highlighted in blue.

The addition of specific targeting functionalities has enabled Mg^{2+} to be visualised directly in organelles via fluorescence microscopy [72–74]. A range of design approaches have been taken – including the use of small molecule sensors [72] and hybrid protein-small molecule systems using HaloTag protein labelling technology [75] – to enable localisation into an organelle of particular interest [73,74]. The latter approach, in particular, offers an extremely versatile targeting strategy and permits long-term cellular retention.

One such interesting example of a small molecule targeted sensor is **Mag-mito** (**Fig. 7F**), which is structurally similar to **Mag-Fura-2**, but instead contains a triazole ring to link a mitochondrial targeting moiety to a fluorescent APTRA-based chelate. To enable cell localisation, the carboxylate binding groups were first protected with acetoxymethylesters, which were subsequently hydrolysed by intracellular esterases after probe uptake (**Section 2.6.3**). The use of **Mag-mito** has provided evidence of Mg^{2+} fluctuations in the mitochondria during the preliminary stages of staurosporine-induced apoptosis in HeLa cells [72]. During

cell apoptosis, it was found that there was an approximate 3-fold increase in 'free' Mg^{2+} to 2.6 mM in comparison to the control experiment with the absence of staurosporine [72].

The use of BODIPY fluorophores has allowed excitation and emission wavelengths to be further red-shifted into the visible range. BODIPY compounds are well known to have high quantum yields, low cytotoxicity and narrow emission and excitation profiles, making them exceptional candidates for use in fluorescence imaging [76]. The core structure also provides an opportunity for further functionalisation and has led to the development of a range of BODIPY-based metal-binding fluorophores [77–79]. Compounds **Mag-B1** (λ_{ex} = 496 nm) and **Mag-B2** (λ_{ex} = 575 nm) are two examples of BODIPY-APTRA probes to detect Mg^{2+}, giving K_d values in the low mM range (4.3 mM for **Mag-B1** and 2.1 mM for **Mag-B2**) (**Fig. 7G** and **Fig. 7H**) [80]. A 'turn-on' response was reported with a 15- and 58-fold increase in the emission intensity for **Mag-B1** and **Mag-B2** respectively upon saturation, due to the inhibition of PET that quenches the fluorescence in the unbound form (**Section 2.6.2**). Red-shifted **Mag-B2** was subsequently studied in live HeLa cells to visualise changes in intracellular 'free' Mg^{2+} (**Fig. 8**) [80].

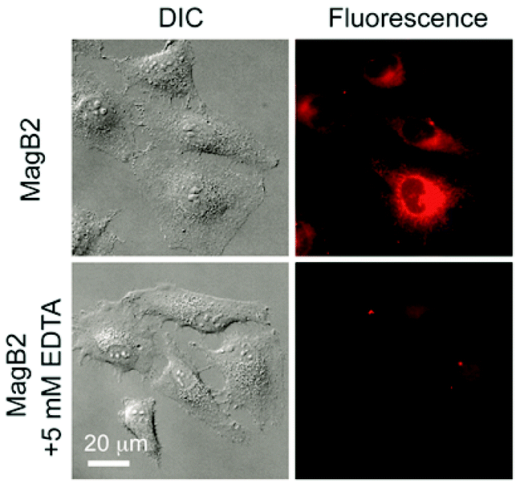

Fig. 8. (*Top*) Fluorescence imaging of Mg^{2+} with **Mag-B2** in live HeLa cells and (*bottom*) with the addition of 5 mM EDTA [80]. Reprinted with permission from [80]. Copyright The Royal Society of Chemistry 2016.

One significant disadvantage of **Mag-B1** and **Mag-B2**, however, is that unlike **Mag-Fura-2** and **Mag-S**, they have a non-ratiometric response to the binding of metal ions. Intracellular artefacts such as photobleaching and dye loading can affect the reliability of such intensity-only probes [80].

Amongst the examples discussed above, changing the fluorophore from the first to the second generation of APTRA probes improves practical aspects such as λ_{ex}, but it does

nothing to improve the intrinsic Mg^{2+} vs Ca^{2+} selectivity profile. In each case, the [5,5,5,5] binding chelate of APTRA binds Ca^{2+} with a higher affinity than Mg^{2+}, in the μM range. Low Ca^{2+} concentrations in most cellular compartments means interference may well be generally small. Nevertheless, to eliminate competitive binding completely, cells have had to be pre-loaded with BAPTA in some studies, to ensure that the observed fluorescence response can be safely attributed to Mg^{2+} alone [80]. For extracellular applications or in cellular compartments where the concentration of 'free' Ca^{2+} is higher, APTRA-based probes are unsuitable for detection of Mg^{2+}, as the probe is fully saturated by competing Ca^{2+} ions.

Lanthanide-based APTRA complexes – a surprising influence on Mg^{2+} vs. Ca^{2+} selectivity

Luminescent lanthanide complexes offer several advantages over conventional fluorophores. They have large pseudo-Stokes' shifts between the absorbance and emission maxima and sharp emission bands [81]. They have unusually long excited state lifetimes (μs – ms) at room temperature, which are not quenched by molecular oxygen, enabling time-gating experiments to be carried out in biological media to eliminate background fluorescence [82,83]. Direct excitation of lanthanide ions is inefficient due to their low molar extinction coefficients, but this limitation can be circumvented by using a strongly-absorbing organic chromophore as a sensitiser [84].

A range of functionalised lanthanide complexes have been developed as probes to bind and respond optically to a number of mono- and di-valent cations [85–89]. The aromatic metal binding unit also acts as the sensitiser. The first example of an APTRA-based lanthanide complex was reported by Parker and co-workers over two-decades ago [86]. Complex **[Ln.L^4]** (**Fig. 9A**) shows μM affinity for both Ca^{2+} and Zn^{2+} ions and low mM affinity for Mg^{2+} [86].

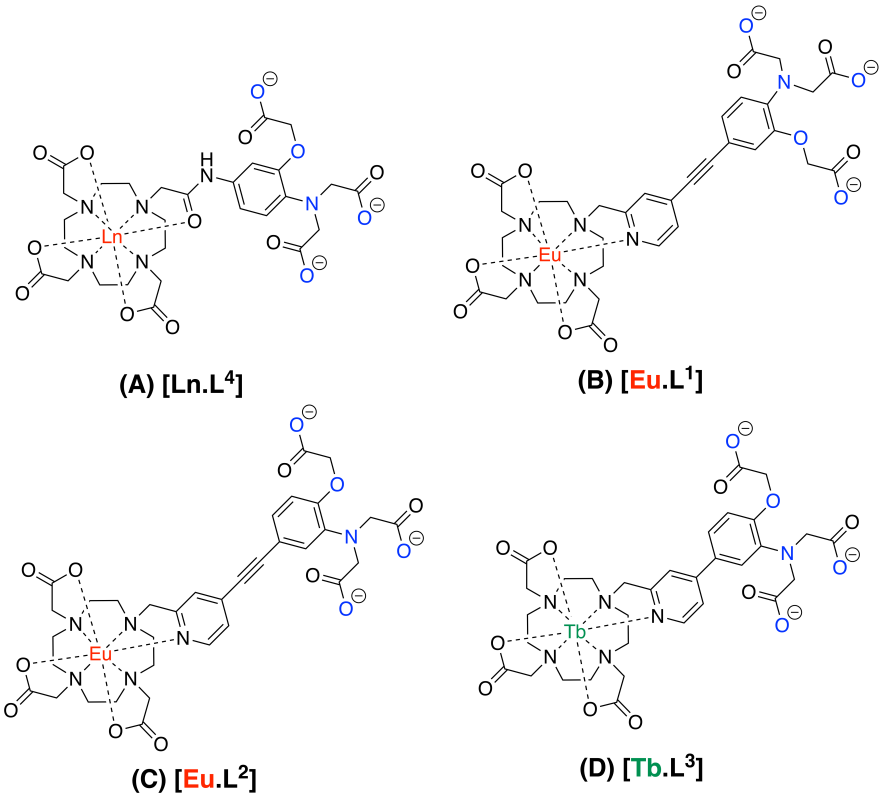

Fig. 9. APTRA-based lanthanide complexes**, [Ln.L^4]**,[86] **[Eu.L^1]**, **[Eu.L^2]** and **[Tb.L^3]** [90]. Binding groups are highlighted in blue.

More recently, APTRA has been incorporated into both a pyridylalkynylaryl, **[Eu.L^1]** and **[Eu.L^2] (Fig. 9B and C)**, and pyridylaryl chromophore **[Tb.L^3]** (**Fig. 9D)**. Both types of complexes are based on an octadentate DOTA-based unit for binding of the Ln^{3+} ion, which forms thermodynamically stable and kinetically inert complexes (DOTA = 1,4,7,10-tetraazacyclododecane-tetraacetate) [90].

Typical of literature examples of luminescent *N-para*-substituted APTRA analogues [63,69–72,80,90], **[Eu.L^1]** displayed a ratiometric response in its excitation spectrum on binding of divalent metal ions due to the elimination of ICT. The intensity of Eu^{3+} emission decreased. In contrast, **[Eu.L^2]** was found to be non-ratiometric, probably due to less significant ICT character from the weaker donor ability of the *para* phenolic oxygen atom, but does show a highly desirable 'turn-on' response in terms of intensity [90].

For each lanthanide complex in this study, a larger luminescent response was reported for the binding of Ca^{2+} and Zn^{2+} ions, attributed to a stronger binding to the aniline nitrogen atom perturbing the ICT state in the absorption spectrum [90].

Remarkably, the relative response towards Mg^{2+}, Ca^{2+} and Zn^{2+} ions was very different compared to other APTRA-based literature examples, including **[Ln.L^4]**, displaying mM affinities for Mg^{2+} and Ca^{2+} and a μM affinity for Zn^{2+}. The highest selectivity was observed from **[Eu.L^2]**, with K_d values of 3.7 mM, 0.9 mM and 53 μM for Mg^{2+}, Ca^{2+} and Zn^{2+} ions respectively [90]. An 18-fold reduction in Ca^{2+} binding affinity was displayed compared to [**Ln.L^4**], and could be due in part to the lower aryl N and O atom donor ability in the push-pull lanthanide systems. Differential solvation effects may also be implicated, with the solvation of the lanthanide complex and/or the metal ion affecting the free energy of complexation [91,92]. The lowest Mg^{2+} affinity in the series was shown by **[Tb.L^3]**, with a K_d of 16.9 mM [90].

Complexes **[Eu.L^1]**, **[Eu.L^2]** and **[Tb.L^3]** are the only known examples of APTRA chelates to exhibit such a high selectivity for Mg^{2+} over Ca^{2+}, and enabled 'free' Mg^{2+} to be measured for the first time in new-born calf serum (NCS) with the 'turn-on' probe **[Eu.L^2]** [90]. A K_d value of 2.4 mM was calculated for Mg^{2+} binding in NCS [90], slightly higher than the known concentration of 'free' Mg^{2+} in healthy human serum (0.7 – 1.1 mM) [93,94].

Although the incorporation of APTRA into lanthanide push-pull systems showed promising results, further work is required in order to increase the excitation wavelength of the chromophore to improve its applications for fluorescence microscopy. The design of a ratiometric probe to measure Mg^{2+} concentrations directly in human serum is also highly desirable.

3.2 Phosphinate ligands – APDAP

A limited number of ligand chelates containing phosphinate groups, –P(O)RO$^-$, as opposed to carboxylates have previously been assessed. Parker and co-workers developed a range of macrocyclic azaphosphinate ligands and studied their complexation with divalent cations (Mg^{2+}, Zn^{2+}, Co^{2+}) and trivalent cations (Fe^{3+} and Ga^{3+} and Ln^{3+}) [95,96]. In 2018 our group developed *o*-aminophenol-*N,N*-diacetate-*O*-methylene-methylphosphinate (APDAP), an APTRA analogue featuring a phosphinate group in place of the phenolate-bound carboxylate [97]. Like APTRA, APDAP is a pentadentate ligand that forms a [5,5,5,5] chelate on binding to divalent metal ions (**Fig. 10A**). The longer C–P and P–O bond lengths mean that the 5-ring chelate containing the phosphinate group has a larger bite angle. Its absorption spectrum is largely insensitive to pH in the physiological range, favouring its potential application as a metal ion probe in cells [97].

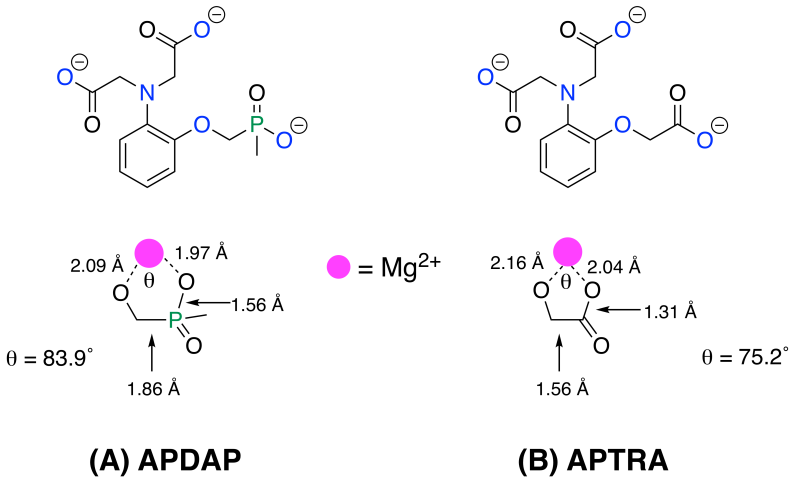

Fig. 10. (A) The structure of APDAP and calculated bond lengths and bite angle (θ) around Mg^{2+}. **(B)** Corresponding bond lengths and bite angle for APTRA bound to Mg^{2+}. Binding groups are in blue.

Absorption spectroscopy was used in the first instance to monitor the binding of divalent metal ions. {The fluorescence associated with the simple aryl chromophore is too weak and the excitation wavelength too short for practicable assessment by fluorescence spectroscopy}. In aqueous solution, the absorption spectrum consisted of one main band at 254 nm with a distinct shoulder at 285 nm. Following binding of Mg^{2+}, the absorbance of the main band decreased and a K_d value of 12.7 mM was calculated, slightly higher than the concentration within cells and serum. In comparison, the binding of Ca^{2+} and Zn^{2+} produced a rather different absorption profile, similar to that observed on protonation, from which it could be tentatively concluded that the aniline nitrogen atom plays a more prominent role in binding to the larger Ca^{2+} and more polarisable Zn^{2+} ions. K_d values of 1.08 mM and 17 μM were calculated for Ca^{2+} and Zn^{2+} respectively (**Fig. 11**). Although there is a 7-fold reduction in Mg^{2+} affinity compared to APTRA, the affinity for both Ca^{2+} and Zn^{2+} was reduced much more – by two to three orders of magnitude. Therefore, *the overall selectivity for Mg^{2+} is significantly improved* [97].

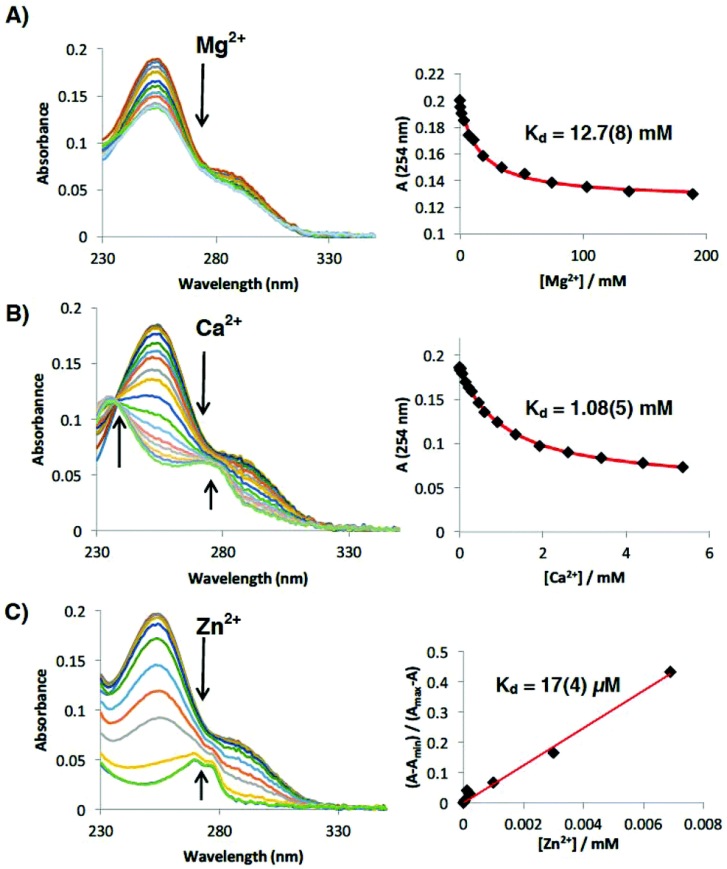

Fig. 11. Absorbance spectra (left) and binding curves with associated fits in red (right) of APDAP following the addition of **(A)** Mg^{2+}, **(B)** Ca^{2+} and **(C)** Zn^{2+} in [HEPES] buffer (50 mM [HEPES], 100 mM [KCl]), pH = 7.21, $T = 298 \pm 3$ K [97]. Reprinted with permission from [97]. Copyright The Royal Society of Chemistry 2018.

A series of DFT calculations was undertaken in order to understand this improved Mg^{2+} selectivity, focusing on the bond lengths and bond angles of APTRA vs. APDAP. Compared to the M–L bond distances determined crystographically by Buccella and co-workers for the Mg^{2+} and Zn^{2+} complexes of APTRA [55], shorter M–L bond lengths were estimated theoretically for the Mg^{2+} complex of APDAP (**Fig. 10**). On the other hand, very little difference in M–L bond lengths was observed between the Zn^{2+} complexes of the two ligands, which were modelled with one H_2O molecule completing the coordination sphere in each case [97].

The lowest energy conformation of 5- and 6-membered chelates is discussed in detail in **Section 2.4** (**Fig. 3**). In the case of APDAP, longer P–O and C–P bond lengths displayed in $[Mg(APDAP)(H_2O)]^-$ (**Fig. 10**), compared to C–O and C–C bonds in $[Mg(APTRA)(H_2O)]^-$, increase the bite angle around the Mg^{2+} ion. This subtle change in donor group affecting cation binding affinities has previously been reported for phosphinate aza-macrocycles [95], and rationalises the higher selectivity demonstrated towards Mg^{2+} ion binding for

phosphinate-based APDAP. The introduction of a phosphinate group gives the 5-membered chelate a larger bite angle (and more akin to that found in a 6-membered chelate), thus inherently favouring the binding of the smaller Mg^{2+} ion.

The APDAP binding framework was subsequently connected to a naphthalene fluorophore in order to provide a means of monitoring the binding of divalent cations via fluorescence spectroscopy, e.g. **Nap.L^3** (**Fig. 12C**) [98]. Similar to the absorption studies of the APDAP unit itself, a significantly higher Mg^{2+} vs. Ca^{2+} selectivity was observed by fluorescence for **Nap.L^3**, compared to carboxylate analogues **Nap.L^1** and **Nap.L^2** (**Fig. 12A** and **B** respectively), enabling the binding of Mg^{2+} to be analysed in competitive media to simulate human serum. For example, dissociation constants of 0.5 mM, 0.4 mM and 3.3 μM were recorded respectively for Mg^{2+}, Ca^{2+} and Zn^{2+} ions and suggest that **Nap.L^3** is more suitable for biological applications than those of the APDAP binding unit alone. Unlike its carboxylate analogues, **Nap.L^3** displayed a non-ratiometric response in the excitation spectrum on Mg^{2+} binding. However, as with the preliminary absorbance binding studies of APDAP, a ratiometric response was observed for Ca^{2+} and Zn^{2+}, again suggesting the aniline nitrogen atom plays a minor role in binding to the smaller Mg^{2+} ions [98].

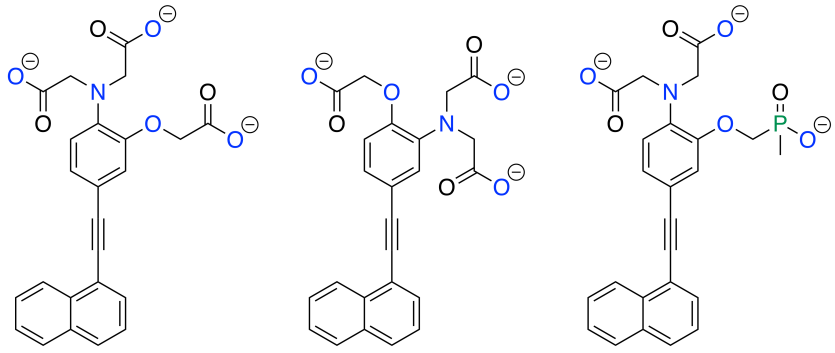

(A) Nap.L^1 **(B) Nap.L^2** **(C) Nap.L^3**

Fig. 12. The structures of APTRA-based **Nap.L^1 (A)**, **Nap.L^2 (B)** and APDAP-based **Nap.L^3**, **(C)**. Binding groups are highlighted in blue

4. Bidentate ligands: β-keto acids

Outlined in **Section 2.5**, it is clear that ligand denticity can be used as a tool to favour the binding of particular metal ions selectively. Over the last two decades, β-keto acids have emerged as a lower denticity alternative to the pentadentate APTRA [5,5,5,5] ligand binding framework. The first set of β-keto acid-functionalised probes to bind Mg^{2+} were reported by London and co-workers in 2001, based on a 4-oxo-4H-quinolizine-3-carboxylic acid binding framework (**Fig. 13A**) [99].

Following this report, Suzuki and Oka have developed a range of β-keto acid-based sensors for fluorescence imaging applications within the so-called KMG series [99 –102]. Bidentate β-keto acids form 6-membered ring chelate structures (**Fig. 13B**). A 6- rather than 5-membered chelate coupled with the lower ligand denticity significantly favours the binding of the smaller Mg^{2+} ion over its larger competitor, Ca^{2+}. The binding of Mg^{2+} is, therefore, more selective. Typically, β-keto acids display a mM affinity for both Mg^{2+} and Ca^{2+} ions, rather than the mM and μM affinities displayed by the majority of APTRA analogues for Mg^{2+} and Ca^{2+}, respectively.

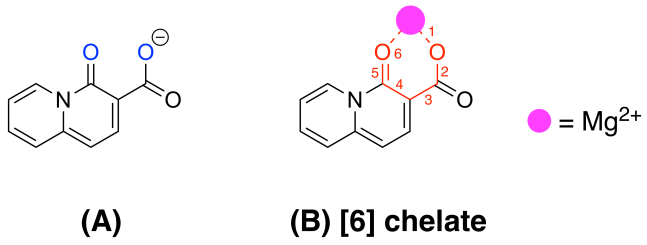

(A) **(B) [6] chelate**

Fig. 13. (A) A bidentate 4-oxo-4H-quinolizine-3-carboxylic acid ligand and **(B)** [6] membered ring chelate formed on metal binding. Donor groups are highlighted in blue.

Another well explored β-diketone group for Mg^{2+} binding is that based on a coumarin fluorophore (for example, **KMG-20**, **Fig. 14A**) [100,101,104]. However, these ligands have not been utilised to the same extent as the 4-oxo-4H-quinolizine-3-carboxylic acid binding framework. Although they typically possess a similarly advantageous mM affinity for Ca^{2+}, the affinity displayed for Mg^{2+} is too weak (most have a K_d > 10 mM). The origin of this difference is possibly the increased electron-donating ability of the nitrogen atom in the quinolizine ring compared to the oxygen in the coumarin system, making the carbonyl donor harder in the former case [101]. Quinolizine-based bidentate binding sites have since been incorporated into a range of fluorophores including, for example, fluorescein (**KMG-104**, **Fig. 14B**) [101] and rhodamine (**KMG-301**, **Fig. 14C**) [102] to give fluorescent 'turn-on' sensors.

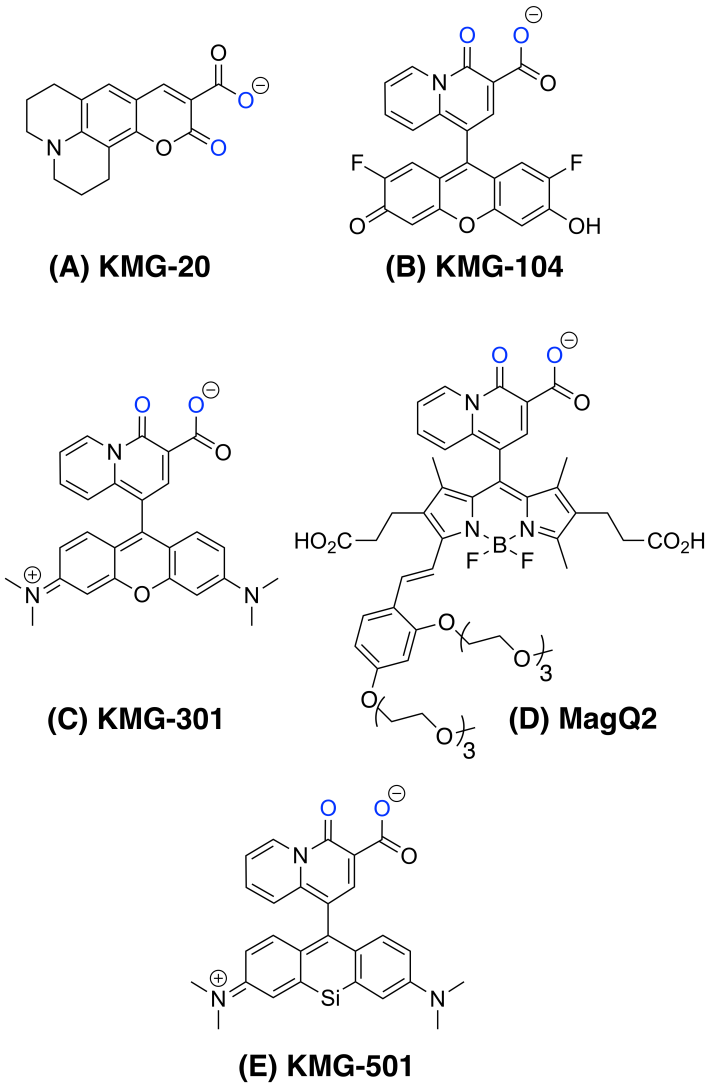

Fig. 14. The structures of the *β*-keto acid probes discussed in this review. Binding groups are highlighted in blue.

A number of fundamental advantages are displayed by the *β*-keto acids compared to the higher dentate APTRA chelators. Most significantly, their superior Mg^{2+} vs Ca^{2+} ion selectivity profile alleviates concerns of co-reporting Ca^{2+} fluxes. However, they too have a number of limitations. Ligands in the KMG series are non-ratiometric, unlike many of the APTRA-based fluorescent sensors, operating via a 'turn-on' PET mechanism, with no wavelength shift on metal ion binding (**Section 2.6.2**). The bidentate binding nature of the *β*-keto acids has also been found to result in the formation of mixed species with Mg^{2+}, forming binary complexes with 'free' Mg^{2+} and ternary complexes with $Mg–ATP^{2-}$ (**Fig. 15**) [17]. Not only was it proven that binding to $Mg–ATP^{2-}$ occurs, but it was also shown that such binding can cause a larger spectral response than binding to 'free' Mg^{2+} ions (**Fig. 15**) [17]. In most cases, simple fluorescence measurements cannot be used to distinguish between the bound and 'free' states of Mg^{2+} that can be formed in the cell, because the K_d

values for both species are in the low mM range (3.8 mM for Mg^{2+}, 14.2 mM for Mg–ATP^{2-}) [17]. So, although it is fair to say that β-keto acids show selectivity for Mg^{2+} over Ca^{2+}, they are not selective for 'free' Mg^{2+}, reducing confidence in the reliability of *in vivo* experiments utilising probes with this ligand.

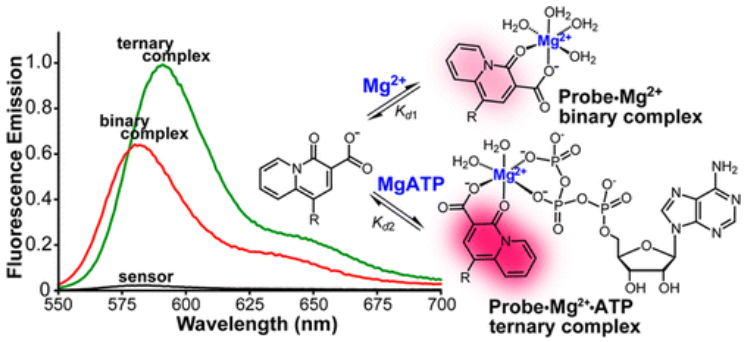

Fig. 15. The emission spectra for the formation of a binary (**probe–Mg^{2+}**) and ternary complex (**probe–Mg–ATP^{2-}**) observed for β-keto acids developed by Buccella and co-workers, R = fluorophore. [17] Reprinted with permission from [17], https://pubs.acs.org/doi/10.1021/ic5000606. Copyright (2014) American Chemical Society. Further permission related to the material excerpted should be directed to the ACS.

Notwithstanding the formation of ternary complexes *in vivo*, there have been a number of recent reports of sensors that feature the 4-oxo-4H-quinolizine-3-carboxylic acid binding framework, in an attempt to try to remedy this shortcoming. Treadwell and co-workers attached a BODIPY fluorophore to a 4-oxo-4H-quinolizine-3-carboxylic acid binding chelate and showed that the spectral response of this turn-on sensor *in vitro* was 5-fold larger for 'free' Mg^{2+} than for Mg–ATP^{2-} [105]. The fluorescence response to 'free' Mg^{2+} and Mg–ATP^{2-} is evidently highly dependent on the system under investigation. But, the selectivity issue remains.

Subsequently, it was shown in work by Buccella and Lin towards the development of **MagQ2** (**Fig. 14D**) that further modification of the BODIPY core with a styryl unit can provide a sensor with the water solubility, appropriate level of lipophilicity and long excitation wavelengths desired for cellular imaging. Furthermore, it was shown that **MagQ2** was capable of monitoring fluxes of 'free' Mg^{2+} in HeLa cells [106].

The most recent report of a quinolizine based sensor, **KMG-501** (a PET-type 'off-on' response, **Fig. 14E**), features a Si-rhodamine unit as the fluorescent platform, and is the first example of a near-infrared (NIR) probe for Mg^{2+} [103]. Such an investigation comes over 20 years after the first NIR sensor for Ca^{2+}, highlighting again how far Mg^{2+} research has lagged behind other divalent metal ions [107]. Oka and co-workers developed a "multi-colour" imaging study, where **KMG-501** was used to monitor changes in 'free' Mg^{2+}, alongside

ATeam and tetramethylrhodamine ethyl ester (TMRE), visualising ATP concentration and mitochondrial membrane depolarisation, respectively (**Fig. 16**). The fluorescence signal emitted from the four fluorophores was monitored from the same cell (**Fig. 16A** and **Fig. 16B**).

Following treatment with FCCP[†], the mitochondrial inner membrane potential decreased dramatically with an increase in cytosolic Mg^{2+}. A gradual decrease in the concentration of cytosolic ATP was also observed (**Fig. 16C**) and weakly correlated with an increase in 'free' Mg^{2+}. No such correlation was seen with the change in mitochondrial inner membrane potential with cytosolic ATP concentration (**Fig. 16D**) [103].

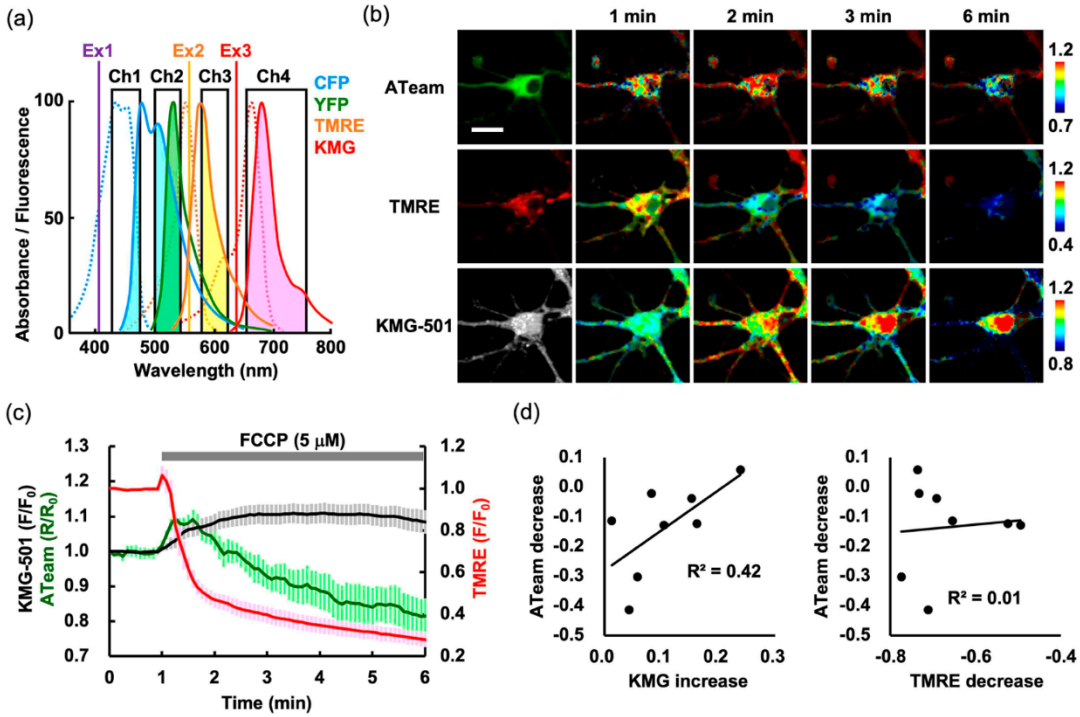

Fig. 16. (A), **(B)** Multi-colour imaging of intracellular Mg^{2+} (**KMG-501**), ATP (CFP and YFP) and mitochondrial inner membrane potential (TMRE), **(C)** Emission of **KMG-501** (*black*), ATeam (*green*) and TMRE (*red*) following treatment with FCCP and **(D)** Correlation between inner mitochondrial membrane potential with **KMG-501** (left) and TMRE (right).[103] Reprinted with permission from [103]. Copyright (2019) American Chemical Society.

This new approach of "multi-colour" imaging provided evidence that β-keto acids could be used to qualitatively monitor changes in 'free' Mg^{2+} *in vivo*. It was assumed that like ATP, the concentration of $Mg–ATP^{2-}$ also decreased, allowing the authors to argue that **KMG-501** was more responsive to changes in 'free' Mg^{2+} than $Mg–ATP^{2-}$ [103].

[†] FCCP (Carbonyl cyanide-*p*-trifluoromethoxyphenylhydrazone) uncouples the mitochondria inner membrane potential inducing the release of 'free' Mg^{2+} into the cytosol [114].

The latest reports on β-keto acid sensors show increasing promise that probes of this nature could be used in the future to reliably monitor 'free' Mg^{2+} fluctuations in cells qualitatively, so as to develop understanding of the role of Mg^{2+} in cell signalling without interference from Ca^{2+}. Yet it is unlikely that these probes will be suitable candidates to quantitively measure 'free' Mg^{2+} concentrations in areas of the body/cell where Ca^{2+} concentrations are above basal levels, because of the interference from Mg-ATP^{2-}. Such interference is likely to be problematic, as in these areas the concentration of Mg-ATP^{2-} is significantly higher than that of 'free' Mg^{2+} ions. Interference from Mg-pyrophosphate is also likely to be problematic, but has not been considered.

Despite much potential, β-keto acid-based systems may, therefore, not solve the problem of monitoring Mg^{2+}. In Ca^{2+}-rich areas, this is particularly apparent, where APTRA chelators are also unsuitable. Alternative ligands/probes are required that are selective for Mg^{2+} over Ca^{2+}, and that will not form ternary complexes *in vivo*. The pentadentate-based **[Eu-L^2]** (**Section 3.1**) and APDAP (**Section 3.2**) that have shown promising initial results could be explored further to this end.

5. The Use of Tridentate Ligands

Only a few examples of Mg^{2+} sensors with a tri- or tetradentate binding chelate have been reported. In 2017, Kikuchi and co-workers described a series of 'turn-off' tridentate fluorescent probes for Mg^{2+} ions. The MGQ series (e.g. **MGQ-2**, **Fig. 17A**) forms one 6- and one 5-membered ring around metal ions (**Fig. 17B**) [108]. The lower denticity and the formation of a [6,5] ring chelate significantly favoured the binding of Mg^{2+} over the larger Ca^{2+}, leading to a high Mg^{2+} vs Ca^{2+} selectivity. Additionally, the shorter M–L bond distances in Mg^{2+} complexes [109] suggest that more rigid binding chelates (such as **MGQ-2**) are highly advantageous to improve selectivity in chelators of a lower denticity. The importance of chelate rigidity demonstrated here is consistent with the findings of Cram [27] and Hancock [37] discussed in **Section 2**: ligand pre-organisation significantly improves the binding affinity and selectivity for metal ions, due to the reduction in conformational flexibility of the free ligand in solution.

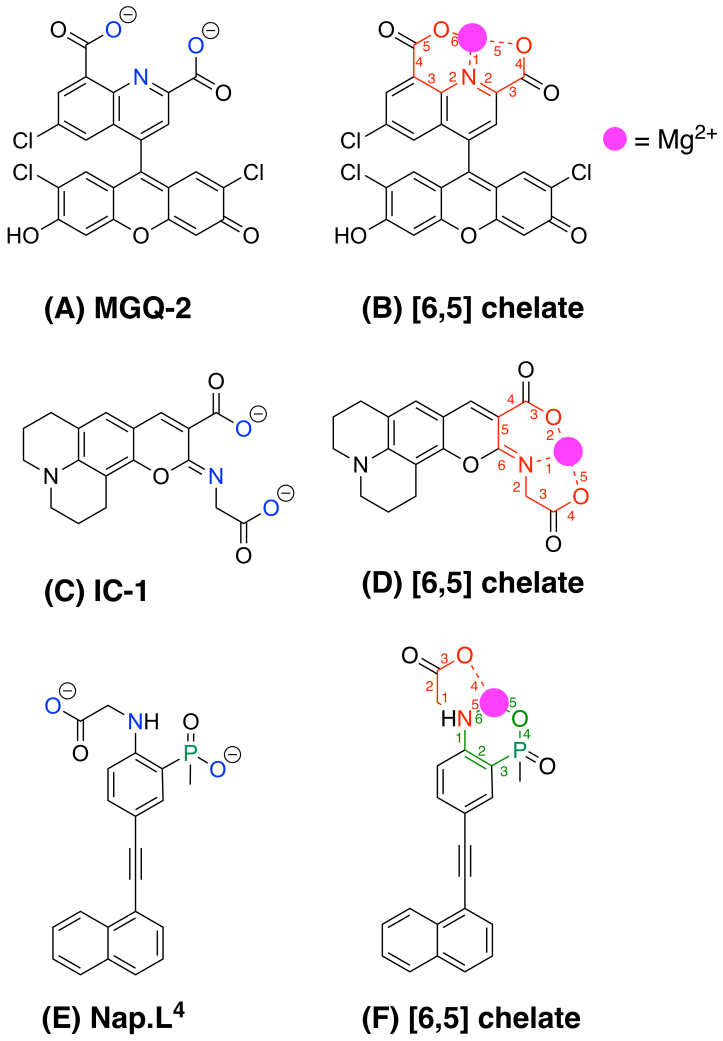

Fig. 17. (A) MGQ-2 developed by Kikuchi and co-workers [108] and **(B)** the [6,5] chelate of on binding of Mg^{2+}, **(C)** A low-affinity Mg^{2+} probe, **Compound A**, [108] and its [6,5] chelate **(D)**. **(E)** The structure of **Nap.L**^{4} and **(F)** the [6,5] chelate on binding to Mg^{2+}. Binding groups are highlighted in blue.

In this study, only the rigid tridentate ligands **MGQ-1** and **MGQ-2** displayed desirable binding properties for Mg^{2+}. For example, **MGQ-2** displayed K_d values of 0.27 mM for Mg^{2+} and 1.5 mM for Ca^{2+}. A 540 nM affinity was calculated for the binding of Zn^{2+} ions. In contrast, a more flexible tridentate iminocoumarin-based chelator **IC-1** (**Fig. 17C**) showed a weak affinity for Mg^{2+}, with very little interference from Ca^{2+}. Increasing the ligand denticity to 4 or 5 improved the binding affinity for both Mg^{2+} and Ca^{2+} ions, but with a poor Mg^{2+} vs. Ca^{2+} selectivity profile [108].

Similarly to bidentate β-keto acids, the formation of ML_2 and MLX complexes with tridentate ligands must also be considered (**Section 2.7** and **4**), a process that is often overlooked in the literature. A binding study of **MGQ-2** with Mg–ATP^{2-} also determined that formation of ternary species is highly probable in solution. A comparable affinity was observed for the

addition of 0.3 – 10 mM of both Mg^{2+} and Mg–ATP^{2-}, with only subtle differences reported in the absorption spectrum in each case. Kikuchi and Mizukami postulated that it is likely that **MGQ-2** binds Mg^{2+} competitively with ATP, due to its small dissociation constant [108]. Subsequent work by the group has seen the combination of 'turn-off' **MGQ-2** and 'turn-on' green fluorescent probe for ratiometric detection of the flux of Mg^{2+} out of HEK293 cells [110].

A tridentate phosphinate-based ligand, **Nap.L^4** has also been examined (**Fig. 17E**) [98]. Similarly to **IC-1**, only very weak binding was observed for Mg^{2+} and Ca^{2+} ions, with negligible fluorescence response. It is possible that the weaker donor effect of the aniline nitrogen postulated in other phosphinate donor systems [97] makes **Nap.L^4** more 'bidentate' in nature. It is also plausible to suggest that the increased flexibility of the ligating donor groups reduced the binding affinity in a similar manner to **IC-1**. Therefore, when lowering the denticity of ligand chelates to bind the smaller Mg^{2+} ion, the rigidity of the binding chelate also needs to be considered in order to maximise affinity and selectivity of binding.

6. Conclusions and Outlook

Over the last decade, a significant amount of research has been undertaken to unlock more detailed information about the role of Mg^{2+} *in vivo*. However, research lags way behind that of other divalent metal ions and, in order to understand Mg^{2+} homeostasis in more detail, a great deal of additional work is required. The relative merits of a number of binding chelates of different denticities have been discussed and analysed, and the different approaches identified that have been undertaken in attempt to bind Mg^{2+} more selectively. It is clear that a binding unit that fulfils all of the desirable quantities for sensing Mg^{2+} *in vivo* is still required. The properties of the main examples of probes discussed in this review are summarised in **Table 3**.

Table 3 Spectroscopic properties of selected pentadentate, tridentate and bidentate probes for 'free' Mg^{2+}.

Probe	Abs λ_{max} (nm)	Emission λ_{max} (nm)	K_d Mg^{2+}	K_d Ca^{2+}	K_d Zn^{2+}	[ref]
Pentadentate – APTRA						
APTRA	254	– [a]	1.8 mM	9.8 μM	10 nM	[55]
Mag–Fura–2	369, 330 [b]	511, 491 [b]	1.9 mM	25 μM	20 nm	[63,111]
Mag–Se	412, 360 [b]	584, 562 [b]	3.3 mM	41 μM	60 nM	[71]
Mag–B2	575, 576 [b]	601 [b]	2.13 mM	15.4 μM	N.D [c]	[80]
[Eu.L^2]	318, 318 [b]	699	3.7 mM	0.9 mM	1.9 μM	[90]
Pentadentate – APDAP						
APDAP	254	– [a]	12.7 mM	1.08 mM	17 μM	[97]
Nap.L^3	350	550, 547 [b]	0.5 mM	0.4 mM	3.3 μM	[98]
Tridentate						
MGQ-2	516	536	0.27 mM	1.5 mM	540 nM	[108]
IC-1	341	507	16.5 mM	N.D [c]	N.D [c]	[108]
Nap.L^4	347	501	N.D [c]	N.D [c]	N.D [c]	[98]
Bidentate						
KMG–20	425, 445 [b]	485, 495 [b]	10 mM	30 mM	N.D [c]	[81]
KMG–104	504	523	2.1 mM	7.5 mM	N.D [c]	[101]
KMG–301	563	590	4.5 mM	N.D [c]	N.D [c]	[102]
MagQ2	516	536	1.5 mM	N.D [c]	N.D [c]	[106]
KMG–501	663	684	3.2 mM	N.D [c]	N.D [c]	[103]

[a] Emission spectra not recorded. [b] Ratiometric sensor, values for the metal–free and Mg^{2+}–bound states respectively. [c] K_d values were not recorded and competitive ML_2 speciation was not considered.

Binding 'free' or labile Mg^{2+} selectively over Ca^{2+} and Zn^{2+} remains the biggest challenge for pentadentate chelates. "Free' Ca^{2+}, for example, has an intracellular concentration of ~100 nM, in contrast to the millimolar concentrations found in extracellular fluids [64]. In contrast, 'free' Zn^{2+} levels are much lower, with transient concentration values ranging from tens to hundreds of pM [112,113]. Higher levels of zinc are found however in certain regions of the body, such as the pancreas and in prostatic fluid. Lanthanide-based [5,5,5,5]-APTRA chelators have been shown to display a high Mg^{2+} vs Ca^{2+} selectivity, far superior to other APTRA probes in the literature. Such an affinity enabled the monitoring of 'free' Mg^{2+} concentrations in NCS for the first time, although the use of a probe with a longer excitation wavelength and that offers ratiometric detection is required for more practicable fluorescence microscopy experiments. A greater understanding of the highly push-pull electronic systems and complex solvation could pave the way for a new generation of push-pull probes for various metal ions.

The development of the [5,5,5,5]-APDAP chelate, a pentadentate analogue of APTRA, has shown that replacing a phenolate-bound carboxylate group with a phosphinate ligand dramatically improved Mg^{2+} selectivity over Ca^{2+} and Zn^{2+}. The affinity for Ca^{2+} was reduced by two orders of magnitude, while the binding of Mg^{2+} was reduced by a factor of only 7 compared to carboxylate based APTRA. Subsequent incorporation into a naphthalene fluorophore similarly demonstrated a better Mg^{2+} vs Ca^{2+} selectivity profile and a sensitivity well suited to cellular 'free' Mg^{2+}. The reduced affinity of **Nap.L[4]** for Ca^{2+} enabled Mg^{2+} binding to be monitored in competitive binding media to mimic human serum, providing encouraging results that APDAP-functionalised luminescent probes could be used in the future to determine concentrations of 'free' Mg^{2+} in Ca^{2+} rich regions of the body.

Lowering the denticity of binding chelates inherently increases the Mg^{2+} vs. Ca^{2+} selectivity profile. Bidentate β-keto acids bind the smaller Mg^{2+} ion in a 6-membered ring chelate, with a higher selectivity compared to the majority of [5,5,5,5] chelate APTRA probes, apart from **LnL[1-3]**. More recently, rigid tridentate probes in the **MQG** series have also been developed with a [6,5] ring chelate around metal ions: they display a high Mg^{2+} vs. Ca^{2+} binding selectivity, but a less favourable 'turn-off' intensity response on metal ion binding. Structurally less rigid tridentate ligands have been found to bind Mg^{2+} or Ca^{2+} efficiently. The binding of Zn^{2+} ions to ligands of lower denticity must also not be forgotten. Although a high nM affinity is greater than the concentration of the majority of 'free' Zn^{2+} in cells, it is worth considering what future changes rigidity and denticity may have on the binding of Zn^{2+} ions, as well as Ca^{2+}, to eliminate any potential competitive binding complications. Tridentate **MGQ-2** displayed a weaker binding affinity for Zn^{2+} than **Mag-Fura-2** (K_d values of 540 nm and 20 nm respectively) [108]. However, the affinity is significantly higher than with the β-keto acid KMG-301, where a negligible fluorescence response was reported for Zn^{2+} binding [102].

Good progress has been made in lowering ligand denticity, but problems still remain with potential competitive binding of phosphorus oxyanions, e.g. $Mg–ATP^{2-}$, leading to the formation of ternary species. Recently, it has been suggested that the fluorescence response observed for $Mg–ATP^{2-}$ is not as significant to that of 'free' Mg^{2+}. However, it is likely to add additional complications for calibration in imaging applications, with some degree of error, if the concentration of 'free' Mg^{2+} is to be determined quantitatively. Ideally, binding should not be competitive between 'free' Mg^{2+} and $Mg–ATP^{2-}$, to ensure the validity of experiments. It should be remembered that $Mg–ATP^{2-}$ is in a significant excess over 'free' Mg^{2+}. Therefore, for further progress to be made in this area, it is not only essential to show

a high Mg^{2+} vs Ca^{2+} selectivity but also important that a high selectivity for 'free' Mg^{2+} is demonstrated.

A tetradentate ligand giving a [6,5,5,5] ring structure, for example, could be an ideal candidate for the future. Such a chelate should favour the binding of Mg^{2+} over Ca^{2+}, whilst simultaneously avoiding any interference from the binding of Mg–ATP^{2-}. The presence of a 6-membered ring chelate will inherently favour Mg^{2+} binding. A ligand chelate with a rigid square planar geometry could be attractive and may significantly reduce the possibility of competitive binding with Mg–ATP^{2-}.

Here through literature examples, we have highlighted a set of coordination chemistry criteria to consider when developing new, highly selective binding chelates for metal ions. The consideration of ligand denticity and the chelate ring size around the metal ion in particular are of critical importance. Approaches outlined in this review are primarily focused on the pursuit of superior binding chelates and fluorescent probes for Mg^{2+} ions. Importantly, however, the key criteria discussed here can also be used to improve the binding selectivity profile of other biologically relevant metal ions.

Conflicts of interest

There are no conflicts to declare.

Acknowledgements

We thank Durham University and EPSRC for support of this work.

References:

[1] A. Romani, Regulation of magnesium homeostasis and transport in mammalian cells, Arch. Biochem. Biophys. 458 (2007) 90–102. https://doi.org/10.1016/j.abb.2006.07.012.

[2] A.M.P. Romani, Cellular magnesium homeostasis, Arch. Biochem. Biophys. 512 (2011) 1–23. https://doi.org/10.1016/j.abb.2011.05.010.

[3] H. Ebel, T. Günther, Magnesium Metabolism: A Review, Clin. Chem. Lab. Med. 18 (1980) 257–270. https://doi.org/10.1515/cclm.1980.18.5.257.

[4] G.A. Rutter, N.J. Osbaldeston, J.G. McCormack, R.M. Denton, Measurement of matrix Mg2+ concentration of rat heart mitochondria using fluorescent probes, Biochem. Soc. Trans. 18 (1990) 894–895. https://doi.org/10.1042/bst0180894.

[5] C.B. Black, H.W. Huang, J.A. Cowan, Biological coordination chemistry of magnesium,

sodium, and potassium ions. Protein and nucleotide binding sites, Coord. Chem. Rev. 135–136 (1994) 165–202. https://doi.org/10.1016/0010-8545(94)80068-5.

[6] J. Šponer, J. Leszczynski, P. Hobza, Hydrogen bonding, stacking and cation binding of DNA bases, J. Mol. Struct. THEOCHEM. 573 (2001) 43–53. https://doi.org/10.1016/S0166-1280(01)00537-1.

[7] A. Romani, A. Scarpa, Regulation of cell magnesium, Arch. Biochem. Biophys. 298 (1992) 1–12. https://doi.org/10.1016/0003-9861(92)90086-C.

[8] M. Tilmann, F. Wolf, Inherited and Acquired Disorders of Magnesium Homeostasis, Curr. Opin. Pediatr. 29 (2017) 187–198. https://doi.org/10.1016/j.physbeh.2017.03.040.

[9] S.M.G. Alghamdi, E.C. Cameron, R. Sutton, Magnesium Deficiency: Pathophysiologic and Clinical Overview, Alllerican J. Kidney Dis. 24 (1994) 737–752.

[10] L.M. Resnick, Ionic basis of hypertension, insulin resistance, vascular disease, and related disorders the mechanism of “syndrome x,” Am. J. Hypertens. 6 (1993) 123S–134S. https://doi.org/10.1093/ajh/6.4S.123S.

[11] J.L. Glick, Dementias: the role of magnesium deficiency and an hypothesis concerning the pathogenesis of Alzheimer’s disease, Med. Hypotheses. 31 (1990) 211–225. https://doi.org/10.1016/0306-9877(90)90095-V.

[12] N. Veronese, A. Zurlo, M. Solmi, C. Luchini, C. Trevisan, G. Bano, E. Manzato, G. Sergi, R. Rylander, Magnesium Status in Alzheimer’s Disease: A Systematic Review, Am. J. Alzheimers. Dis. Other Demen. 31 (2016) 208–213. https://doi.org/10.1177/1533317515602674.

[13] A. Tin, M. Grams, M. Maruthur, B. Astor, D. Couper, T. Mosley, E. Selvin, J. Coresh, W. Kao, Results from the Atherosclerosis Risk in Communities study suggest that low serum magnesium is associated with incident kidney disease, Kidney Int. 87 (2015) 820–827. https://doi.org/10.1038/ki.2014.331.Results.

[14] W. Hasselbach, DIE BINDUNG VON ADENOSINDIPHOSPHAT, VON ANORGANISCHEM PHOSPHAT UND VON ERDALKALIEN AN DIE STRUKTURPROTEINE DES MUSKELS, Biochim. Biophys. Acta. 25 (1957) 562–574. https://doi.org/10.1016/0006-3002(57)90528-0.

[15] V. Trapani, G. Farruggia, C. Marraccini, S. Iotti, A. Cittadini, F.I. Wolf, Intracellular magnesium detection: Imaging a brighter future, Analyst. 135 (2010) 1855–1866. https://doi.org/10.1039/c0an00087f.

[16] C. Feillet-Coudray, C. Coudray, The Stable Isotope Use in the Exploration of Bioavailability and Metabolism of Magnesium, Curr. Nutr. Food Sci. 1 (2005) 63–70. https://doi.org/10.2174/1573401052953212.

[17] S.C. Schwartz, B. Pinto-Pacheco, J.P. Pitteloud, D. Buccella, Formation of ternary complexes with MgATP: Effects on the detection of Mg2+ in biological samples by bidentate fluorescent sensors, Inorg. Chem. 53 (2014) 3204–3209. https://doi.org/10.1021/ic5000606.

[18] T.S. Lazarou, D. Buccella, Advances in imaging of understudied ions in signaling: A focus on magnesium, Curr. Opin. Chem. Biol. 57 (2020) 27–33. https://doi.org/10.1016/j.cbpa.2020.04.002.

[19] J.E. DiCiccio, B.E. Steinberg, Lysosomal pH and analysis of the counter ion pathways that support acidification, J. Gen. Physiol. 137 (2011) 385–390. https://doi.org/10.1085/jgp.201110596.

[20] P. Thordarson, Determining association constants from titration experiments in supramolecular chemistry, Chem. Soc. Rev. 40 (2011) 1305–1323. https://doi.org/10.1039/c0cs00062k.

[21] K. Kaur, R. Saini, A. Kumar, V. Luxami, N. Kaur, P. Singh, S. Kumar, Chemodosimeters: An approach for detection and estimation of biologically and medically relevant metal ions, anions and thiols, Coord. Chem. Rev. 256 (2012) 1992–2028. https://doi.org/10.1016/j.ccr.2012.04.013.

[22] R.G. Pearson, Hard and Soft Acids and Bases, J. Am. Chem. Soc. 85 (1963) 3533–3539. https://doi.org/10.1021/ja00905a001.

[23] R.G. Pearson, Hard and soft acids and bases, HSAB, part I: Fundamental principles, J. Chem. Educ. 45 (1968) 581–587. https://doi.org/10.1021/ed045p581.

[24] J.J.R. Fraústo Da Silva, The chelate effect redefined, J. Chem. Educ. 60 (1983) 390–392. https://doi.org/10.1021/ed060p390.

[25] P. Atkins, T. Overton, J. Rourke, M. Weller, F. Armstrong, Inorganic Chemistry, Fifth Edit, Oxford University Press, 2010.

[26] C.S. Chung, Entropy effects in chelation reactions, J. Chem. Educ. 61 (1984) 1062–1064. https://doi.org/10.1021/ed061p1062.

[27] D.J. Cram, The Design of Molecular Hosts, Guests, and Their Complexes (Nobel Lecture), Angew. Chem. Int. Ed. Engl. 27 (1988) 1009–1112.

[28] S.J. Archibald, Coordination chemistry of macrocyclic ligands, Annu. Reports Prog. Chem. - Sect. A. 105 (2009) 297–322. https://doi.org/10.1039/b818281g.

[29] J. Li, D. Yim, W.D. Jang, J. Yoon, Recent progress in the design and applications of fluorescence probes containing crown ethers, Chem. Soc. Rev. 46 (2017) 2437–2458. https://doi.org/10.1039/c6cs00619a.

[30] A. Sargenti, G. Farruggia, N. Zaccheroni, C. Marraccini, M. Sgarzi, C. Cappadone, E. Malucelli, A. Procopio, L. Prodi, M. Lombardo, S. Lotti, Synthesis of a highly Mg 2+-selective fluorescent probe and its application to quantifying and imaging total intracellular magnesium, Nat. Protoc. 12 (2017) 461–471. https://doi.org/10.1038/nprot.2016.183.

[31] R.D. Hancock, Chelate ring size and metal ion selection: The basis of selectivity for metal ions in open-chain ligands and macrocycles, J. Chem. Educ. 69 (1992) 615–621. https://doi.org/10.1021/ed069p615.

[32] R.D. Hancock, A.E. Martell, Ligand Design for Selective Complexation of Metal Ions in Aqueous Solution, Chem. Rev. 89 (1989) 1875–1914. https://doi.org/10.1021/cr00098a011.

[33] R.D. Hancock, The pyridyl group in ligand design for selective metal ion complexation and sensing, Chem. Soc. Rev. 42 (2013) 1500–1524. https://doi.org/10.1039/c2cs35224a.

[34] R.D. Shannon, Revised effective ionic radii and systematic studies of interatomic distances in halides and chalcogenides, Acta Crystallogr. Sect. A. 32 (1976) 751–767. https://doi.org/10.1107/S0567739476001551.

[35] A.E. Martell, R.M. Smith, Critical Stability Constants, Springer US, 1974. https://doi.org/10.1007/978-1-4615-6761-5.

[36] R.D. Hancock, L.J. Bartolotti, A DFT analysis of the effect of chelate ring size on metal ion selectivity in complexes of polyamine ligands, Polyhedron. 52 (2013) 284–293. https://doi.org/10.1016/j.poly.2012.09.031.

[37] R.D. Hancock, The pyridyl group in ligand design for selective metal ion complexation and sensing, Chem. Soc. Rev. 42 (2013) 1500–1524. https://doi.org/10.1039/c2cs35224a.

[38] M. Bazargan, M. Mirzaei, A. Franconetti, A. Frontera, On the preferences of five-membered

chelate rings in coordination chemistry: Insights from the Cambridge Structural Database and theoretical calculations, Dalt. Trans. 48 (2019) 5476–5490. https://doi.org/10.1039/c9dt00542k.

[39] M. Brady, S.D. Piombo, C. Hu, D. Buccella, Structural and spectroscopic insight into the metal binding properties of the o-aminophenol-N,N,O-triacetic acid (APTRA) chelator: implications for design of metal indicators, Dalt. Trans. 45 (2016) 12458–12464. https://doi.org/10.1039/C6DT01557C.

[40] D.I. Pattison, M.J. Davies, Actions of ultraviolet light on cellular structures., EXS. (2006) 131–157. https://doi.org/10.1007/3-7643-7378-4_6.

[41] E. Baggaley, J.A. Weinstein, J.A.G. Williams, Lighting the way to see inside the live cell with luminescent transition metal complexes, Coord. Chem. Rev. 256 (2012) 1762–1785. https://doi.org/10.1016/J.CCR.2012.03.018.

[42] A.P. de Silva, H.Q.N. Gunaratne, T. Gunnlaugsson, A.J.M. Huxley, C.P. McCoy, J.T. Rademacher, T.E. Rice, Signaling Recognition Events with Fluorescent Sensors and Switches, Chem. Rev. 97 (1997) 1515–1566. https://doi.org/10.1021/cr960386p.

[43] A.T. Aron, M.O. Loehr, J. Bogena, C.J. Chang, An Endoperoxide Reactivity-Based FRET Probe for Ratiometric Fluorescence Imaging of Labile Iron Pools in Living Cells, J. Am. Chem. Soc. 138 (2016) 14338–14346. https://doi.org/10.1021/jacs.6b08016.

[44] C.Y.S. Chung, J.M. Posimo, S. Lee, T. Tsang, J.M. Davis, D.C. Brady, C.J. Chang, Activity-based ratiometric FRET probe reveals oncogene-driven changes in labile copper pools induced by altered glutathione metabolism, Proc. Natl. Acad. Sci. U. S. A. 116 (2019) 18285–18294. https://doi.org/10.1073/pnas.1904610116.

[45] S. Xu, H. Liu, L. Chen, J. Yuan, Y. Liu, L. Teng, S. Huan, L. Yuan, X. Zhang, W. Tan, Learning from Artemisinin: Bioinspired Design of a Reaction-Based Fluorescent Probe for the Selective Sensing of Labile Heme in Complex Biosystems, (2020). https://doi.org/10.1021/jacs.9b11245.

[46] M.H. Lee, J.S. Kim, J.L. Sessler, Small molecule-based ratiometric fluorescence probes for cations, anions, and biomolecules, Chem. Soc. Rev. 44 (2015) 4185–4191. https://doi.org/10.1039/c4cs00280f.

[47] A.P. De Silva, T.S. Moody, G.D. Wright, Fluorescent PET (Photoinduced Electron Transfer) sensors as potent analytical tools, Analyst. 134 (2009) 2385–2393. https://doi.org/10.1039/b912527m.

[48] B. Daly, J. Ling, A.P. De Silva, Current developments in fluorescent PET (photoinduced electron transfer) sensors and switches, Chem. Soc. Rev. 44 (2015) 4203–4211. https://doi.org/10.1039/c4cs00334a.

[49] K.P. Carter, A.M. Young, A.E. Palmer, Fluorescent sensors for measuring metal ions in living systems, Chem. Rev. 114 (2014) 4564–4601. https://doi.org/10.1021/cr400546e.

[50] M. Liu, X. Yu, M. Li, N. Liao, A. Bi, Y. Jiang, S. Liu, Z. Gong, W. Zeng, Fluorescent probes for the detection of magnesium ions (Mg2+): From design to application, RSC Adv. 8 (2018) 12573–12587. https://doi.org/10.1039/c8ra00946e.

[51] R.Y. Tsien, A non-disruptive technique for loading calcium buffers and indicators into cells, Nature. 290 (1981) 527–528. https://doi.org/10.1038/290527a0.

[52] Y. Zhang, L.-C. Yu, Single-cell microinjection technology in cell biology, BioEssays. 30 (2008) 606–610. https://doi.org/10.1002/bies.20759.

[53] S. Lee, J. Xie, X. Chen, Peptide-based probes for targeted molecular imaging, Biochemistry. 49 (2010) 1364–1376. https://doi.org/10.1021/bi901135x.

[54] E.W. Miller, L. Zeng, D.W. Domaille, C.J. Chang, Preparation and use of Coppersensor-1, a synthetic fluorophore for live-cell copper imaging, Nat. Protoc. 1 (2006) 824–827. https://doi.org/10.1038/nprot.2006.140.

[55] M. Brady, S.D. Piombo, C. Hu, D. Buccella, Structural and spectroscopic insight into the metal binding properties of the: O -aminophenol- N, N, O -triacetic acid (APTRA) chelator: Implications for design of metal indicators, Dalt. Trans. 45 (2016) 12458–12464. https://doi.org/10.1039/c6dt01557c.

[56] V.L. Pecoraro, J.D. Hermes, W.W. Cleland, Stability Constants of Mg2+ and Cd2+ Complexes of Adenine Nucleotides and Thionucleotides and Rate Constants for Formation and Dissociation of MgATP and MgADP, Biochemistry. 23 (1984) 5262–5271. https://doi.org/10.1021/bi00317a026.

[57] S.M. Lambert, J.I. Watters, The Complexes of Magnesium Ion with Pyrophosphate and Triphosphate Ions, J. Am. Chem. Soc. 79 (1957) 5606–5608. https://doi.org/10.1021/ja01578a006.

[58] A.K. Covington, E.Y. Danish, Measurement of magnesium stability constants of biologically relevant ligands by Simultaneous use of pH and ion-selective electrodes, J. Solution Chem. 38 (2009) 1449–1462. https://doi.org/10.1007/s10953-009-9459-3.

[59] R.S. Mulla, M.S. Beecroft, R. Pal, J.A. Aguilar, J. Pitarch-Jarque, E. García-España, E. Lurie-Luke, G.J. Sharples, J.A. Gareth Williams, On the Antibacterial Activity of Azacarboxylate Ligands: Lowered Metal Ion Affinities for Bis-amide Derivatives of EDTA do not mean Reduced Activity, Chem. - A Eur. J. 24 (2018) 7137–7148. https://doi.org/10.1002/chem.201800026.

[60] R.Y. Tsien, New Calcium Indicators and Buffers with High Selectivity Against Magnesium and Protons: Design, Synthesis, and Properties of Prototype Structures, Biochemistry. 19 (1980) 2396–2404. https://doi.org/10.1021/bi00552a018.

[61] G. Grynkiewicz, M. Poenie, R.Y. Tsien, A new generation of Ca2+ indicators with greatly improved fluorescence properties, J. Biol. Chem. 260 (1985) 3440–3450.

[62] L.A. Levy, E. Murphy, B. Raju, R.E. London, Measurement of Cytosolic Free Magnesium Ion Concentration by19F NMR, Biochemistry. 27 (1988) 4041–4048. https://doi.org/10.1021/bi00411a021.

[63] B. Raju, E. Murphy, L.A. Levy, R.D. Hall, R.E. London, A fluorescent indicator for measuring cytosolic free magnesium, Am. J. Physiol. - Cell Physiol. 256 (1989) 540–548. https://doi.org/10.1152/ajpcell.1989.256.3.c540.

[64] D.E. Clapham, Calcium Signaling, Cell. 131 (2007) 1047–1058. https://doi.org/10.1016/j.cell.2007.11.028.

[65] F.L. Bygrave, A. Benedetti, What is the concentration of calcium ions in the endoplasmic reticulum?, Cell Calcium. 19 (1996) 547–551. https://doi.org/10.1016/S0143-4160(96)90064-0.

[66] S. Samtleben, J. Jaepel, C. Fecher, T. Andreska, M. Rehberg, R. Blum, Direct imaging of ER calcium with targeted-esterase induced dye loading (TED), J. Vis. Exp. (2013) 1–17. https://doi.org/10.3791/50317.

[67] J. Suzuki, K. Kanemaru, M. Iino, Genetically Encoded Fluorescent Indicators for Organellar Calcium Imaging, Biophys. J. 111 (2016) 1119–1131. https://doi.org/10.1016/j.bpj.2016.04.054.

[68] ThermoFisher, Introduction to Fluorescence Techniques Molecular Probes ™ Handbook A Guide to Fluorescent Probes and Labeling Technologies, 11th Editi, 2010. www.invitrogen.com/probes.

[69] P.A. Otten, R.E. London, L.A. Levy, A new approach to the synthesis of APTRA indicators, Bioconjug. Chem. 12 (2001) 76–83. https://doi.org/10.1021/bc000069w.

[70] G. Zhang, D. Jacquemin, D. Buccella, Tuning the Spectroscopic Properties of Ratiometric Fluorescent Metal Indicators: Experimental and Computational Studies on Mag-fura-2 and Analogues, J. Phys. Chem. B. 121 (2017) 696–705. https://doi.org/10.1021/acs.jpcb.6b11045.

[71] M.S. Afzal, J.P. Pitteloud, D. Buccella, Enhanced ratiometric fluorescent indicators for magnesium based on azoles of the heavier chalcogens, Chem. Commun. 50 (2014) 11358–11361. https://doi.org/10.1039/c4cc04460f.

[72] G. Zhang, J.J. Gruskos, M.S. Afzal, D. Buccella, Visualizing changes in mitochondrial Mg2+ during apoptosis with organelle-targeted triazole-based ratiometric fluorescent sensors, Chem. Sci. 6 (2015) 6841–6846. https://doi.org/10.1039/c5sc02442k.

[73] J.J. Gruskos, G. Zhang, D. Buccella, Visualizing Compartmentalized Cellular Mg2+ on Demand with Small-Molecule Fluorescent Sensors, J. Am. Chem. Soc. 138 (2016) 14639–14649. https://doi.org/10.1021/jacs.6b07927.

[74] Y. Matsui, Y. Funato, H. Imamura, H. Miki, S. Mizukami, K. Kikuchi, Visualization of long-term Mg2+ dynamics in apoptotic cells using a novel targetable fluorescent probe, Chem. Sci. 8 (2017) 8255–8264. https://doi.org/10.1039/c7sc03954a.

[75] G. V. Los, L.P. Encell, M.G. McDougall, D.D. Hartzell, N. Karassina, C. Zimprich, M.G. Wood, R. Learish, R.F. Ohana, M. Urh, D. Simpson, J. Mendez, K. Zimmerman, P. Otto, G. Vidugiris, J. Zhu, A. Darzins, D.H. Klaubert, R.F. Bulleit, K. V. Wood, HaloTag: A novel protein labeling technology for cell imaging and protein analysis, ACS Chem. Biol. 3 (2008) 373–382. https://doi.org/10.1021/cb800025k.

[76] A. Loudet, K. Burgess, BODIPY dyes and their derivatives: Syntheses and spectroscopic properties, Chem. Rev. 107 (2007) 4891–4932. https://doi.org/10.1021/cr078381n.

[77] P. Batat, G. Vives, R. Bofinger, R.W. Chang, B. Kauffmann, R. Oda, G. Jonusauskas, N.D. McClenaghan, Dynamics of ion-regulated photoinduced electron transfer in BODIPY-BAPTA conjugates, Photochem. Photobiol. Sci. 11 (2012) 1666–1674. https://doi.org/10.1039/c2pp25130b.

[78] J.L. Bricks, A. Kovalchuk, C. Trieflinger, M. Nofz, M. Büschel, A.I. Tolmachev, J. Daub, K. Rurack, On the development of sensor molecules that display FeIII- amplified fluorescence, J. Am. Chem. Soc. 127 (2005) 13522–13529. https://doi.org/10.1021/ja050652t.

[79] N. Basaric, M. Baruah, W. Quin, B. Metten, M. Smet, W. Dehaen, N. Boens, Synthesis and spectroscopic characterisation of BODIPY R? based fluorescent off–on indicators with low affinity for calcium, Org. Biomol. Chem. 3 (2005) 2755–2761. https://doi.org/10.1016/S0020-1693(00)90282-2.

[80] Q. Lin, J.J. Gruskos, D. Buccella, Bright, red emitting fluorescent sensor for intracellular imaging of Mg2+, Org. Biomol. Chem. 14 (2016) 11381–11388. https://doi.org/10.1039/c6ob02177h.

[81] N. Hamon, A. Roux, M. Beyler, J. Mulatier, C. Nguyen, M. Maynadier, N. Bettache, A. Duperray, A. Grichine, S. Brasselet, M. Gary-bobo, O. Maury, R. Tripier, N. Hamon, A. Roux, M. Beyler, J. Mulatier, C. Andraud, in vitro and in vivo one- and two-photon bioimaging applications . Pyclen based Ln (III) complexes as highly luminescent bioprobes for in vitro and in vivo one- and two-photon bioimaging applications ., (2020). https://doi.org/10.1021/jacs.0c03496.

[82] E. Soini, I. Hemmit, Fluoroimmunoassay : Present Status and Key Problems, Methods. 25 (1979) 353–361.

[83] A.T. Frawley, R. Pal, D. Parker, Very bright, enantiopure europium(III) complexes allow time-gated chiral contrast imaging, Chem. Commun. 52 (2016) 13349–13352. https://doi.org/10.1039/c6cc07313a.

[84] J.C.G. Bünzli, C. Piguet, Taking advantage of luminescent lanthanide ions, Chem. Soc. Rev. 34 (2005) 1048–1077. https://doi.org/10.1039/b406082m.

[85] O. Reany, T. Gunnlaugsson, D. Parker, Selective signalling of zinc ions by modulation of terbium luminescence, Chem. Commun. (2000) 473–474. https://doi.org/10.1039/b000283f.

[86] O. Reany, T. Gunnlaugsson, D. Parker, A model system using modulation of lanthanide luminescence to signal Zn2+ in competitive aqueous media, J. Chem. Soc. Perkin Trans. 2. (2000) 1819–1831. https://doi.org/10.1039/b003963m.

[87] S.J.A. Pope, R.H. Laye, Design, synthesis and photophysical studies of an emissive, europium based, sensor for zinc, Dalt. Trans. 44 (2006) 3108–3113. https://doi.org/10.1039/b605837j.

[88] C. Rivas, G.J. Stasiuk, M. Sae-Heng, N.J. Long, Towards understanding the design of dual-modal MR/fluorescent probes to sense zinc ions, Dalt. Trans. 44 (2015) 4976–4985. https://doi.org/10.1039/c4dt02981j.

[89] A.K.R. Junker, M. Tropiano, S. Faulkner, T.J. Sørensen, Kinetically Inert Lanthanide Complexes as Reporter Groups for Binding of Potassium by 18-crown-6, Inorg. Chem. 55 (2016) 12299–12308. https://doi.org/10.1021/acs.inorgchem.6b02063.

[90] E.R.H. Walter, J.A.G. Williams, D. Parker, APTRA-Based Luminescent Lanthanide Complexes Displaying Enhanced Selectivity for Mg2+, Chem. - A Eur. J. 24 (2018) 7724–7733. https://doi.org/10.1002/chem.201800745.

[91] G. Schreckenbach, Differential Solvation, Chem. - A Eur. J. 23 (2017) 3797–3803. https://doi.org/10.1002/chem.201604075.

[92] T. Riis-Johannessen, N.D. Favera, T.K. Todorova, S.M. Huber, L. Gagliardi, C. Piguet, Understanding, controlling and programming cooperativity in self-assembled polynuclear complexes in solution, Chem. - A Eur. J. 15 (2009) 12702–12718. https://doi.org/10.1002/chem.200900904.

[93] F.W. Lowenstein, M.F. Stanton, Serum Magnesium Levels in The United States, 1971-1974, J. Am. Coll. Nutr. 5 (1986) 399–414. https://doi.org/10.1080/07315724.1986.10720143.

[94] J.H.F. de Baaij, J.G.J. Hoenderop, R.J.M. Bindels, Magnesium in man: Implications for health and disease, Physiol. Rev. 95 (2015) 1–46. https://doi.org/10.1152/physrev.00012.2014.

[95] E. Cole, R.C.B. Copley, J.A.K. Howard, D. Parker, G. Ferguson, J.F. Gallagher, B. Kaitner, A. Harrison, L. Royale, 1,4,7-Triazacyclononane-l,4,7-triyltrimethylenetris- (phenylphosphinate) enforces Octahedral Geometry: Crystal and Solution Structures of its Metal Complexes and Comparative Biodistribution Studies of Radiolabeled Indium and Gallium Complexes, J. Chem. Soc. Perkin Trans. (1994) 1619–1629. https://doi.org/10.1017/CBO9781107415324.004.

[96] C.J. Broan, K.J. Jankowski, R. Kataky, D. Parker, Synthesis and Complex Stability of Parent and C-Functionalised Derivatives of 1,4,7-Triazacyclononane-1,4,7-tris[methylene(methylphosphinic acid)]: an Effective New Complexing Agent, (1990) 1738–1739. https://doi.org/10.1039/C39900001738.

[97] E.R.H. Walter, M.A. Fox, D. Parker, J.A.G. Williams, Enhanced selectivity for Mg2+with a phosphinate-based chelate: APDAP: versus APTRA, Dalt. Trans. 47 (2018) 1879–1887. https://doi.org/10.1039/c7dt04698g.

[98] E.R.H. Walter, J.A.G. Williams, D. Parker, Tuning Mg(II) Selectivity: Comparative Analysis of the Photophysical Properties of Four Fluorescent Probes with an Alkynyl-Naphthalene

Fluorophore, Chem. - A Eur. J. 24 (2018) 6432–6441. https://doi.org/10.1002/chem.201800013.

[99] P.A. Otten, R.E. London, L.A. Levy, 4-Oxo-4H-quinolizine-3-carboxylic acids as Mg2+ selective, fluorescent indicators, Bioconjug. Chem. 12 (2001) 203–212. https://doi.org/10.1021/bc000087d.

[100] Y. Suzuki, H. Komatsu, T. Ikeda, N. Saito, S. Araki, D. Citterio, H. Hisamoto, Y. Kitamura, T. Kubota, J. Nakagawa, K. Oka, K. Suzuki, Design and synthesis of Mg2+-selective fluoroionophores based on a coumarin derivative and application for Mg2+ measurement in a living cell, Anal. Chem. 74 (2002) 1423–1428. https://doi.org/10.1021/ac010914j.

[101] H. Komatsu, N. Iwasawa, D. Citterio, Y. Suzuki, T. Kubota, K. Tokuno, Y. Kitamura, K. Oka, K. Suzuki, Design and synthesis of highly sensitive and selective fluorescein-derived magnesium fluorescent probes and application to intracellular 3D Mg2+ imaging, J. Am. Chem. Soc. 126 (2004) 16353–16360. https://doi.org/10.1021/ja049624l.

[102] Y. Shindo, T. Fujii, H. Komatsu, D. Citterio, K. Hotta, K. Suzuki, K. Oka, Newly developed Mg2+-selective fluorescent probe enables visualization of Mg2+ dynamics in mitochondria, PLoS One. 6 (2011). https://doi.org/10.1371/journal.pone.0023684.

[103] O. Murata, Y. Shindo, Y. Ikeda, N. Iwasawa, D. Citterio, K. Oka, Y. Hiruta, Near-Infrared Fluorescent Probes for Imaging of Intracellular Mg2+ and Application to Multi-Color Imaging of Mg2+, ATP, and Mitochondrial Membrane Potential, Anal. Chem. (2019). https://doi.org/10.1021/acs.analchem.9b03872.

[104] V.K. Gupta, N. Mergu, L.K. Kumawat, A.K. Singh, Selective naked-eye detection of Magnesium (II) ions using a coumarin-derived fluorescent probe, Sensors Actuators, B Chem. 207 (2015) 216–223. https://doi.org/10.1016/j.snb.2014.10.044.

[105] R. Treadwell, F. De Moliner, R. Subiros-Funosas, T. Hurd, K. Knox, M. Vendrell, A fluorescent activatable probe for imaging intracellular Mg2+, Org. Biomol. Chem. 16 (2018) 239–244. https://doi.org/10.1039/c7ob02965a.

[106] Q. Lin, D. Buccella, Highly selective, red emitting BODIPY-based fluorescent indicators for intracellular Mg2+ imaging, J. Mater. Chem. B. 6 (2018) 7247–7256. https://doi.org/10.1039/c8tb01599f.

[107] E.U. Akkaya, S. Turkyilmaz, A squaraine-based near IR fluorescent chemosensor for calcium, Tetrahedron Lett. 38 (1997) 4513–4516. https://doi.org/10.1016/S0040-4039(97)00917-9.

[108] Y. Matsui, K.K. Sadhu, S. Mizukami, K. Kikuchi, Highly selective tridentate fluorescent probes for visualizing intracellular Mg2+ dynamics without interference from Ca2+ fluctuation, Chem. Commun. 53 (2017) 10644–10647. https://doi.org/10.1039/c7cc06141b.

[109] M.E. Maguire, J.A. Cowan, Magnesium chemistry and biochemistry, BioMetals. 15 (2002) 203–210. https://doi.org/10.1023/A:1016058229972.

[110] Y. Matsui, S. Mizukami, K. Kikuchi, Ratiometric imaging of intracellular Mg2+ dynamics using a red fluorescent turn-off probe and a green fluorescent turn-on probe, Chem. Lett. 47 (2018) 23–26. https://doi.org/10.1246/cl.170918.

[111] T.J.B. Simons, Measurement of free Zn2+ ion concentration with the fluorescent probe mag-fura-2 (furaptra), J. Biochem. Biophys. Methods. 27 (1993) 25–37. https://doi.org/10.1016/0165-022X(93)90065-V.

[112] A. Krężel, W. Maret, Zinc-buffering capacity of a eukaryotic cell at physiological pZn, J. Biol. Inorg. Chem. 11 (2006) 1049–1062. https://doi.org/10.1007/s00775-006-0150-5.

[113] W. Maret, Zinc in cellular regulation: The nature and significance of “zinc signals,” Int. J. Mol.

Sci. 18 (2017). https://doi.org/10.3390/ijms18112285.

[114] T. Kubota, Y. Shindo, K. Tokuno, H. Komatsu, H. Ogawa, S. Kudo, Y. Kitamura, K. Suzuki, K. Oka, Mitochondria are intracellular magnesium stores: Investigation by simultaneous fluorescent imagings in PC12 cells, Biochim. Biophys. Acta - Mol. Cell Res. 1744 (2005) 19–28. https://doi.org/10.1016/j.bbamcr.2004.10.013.